

Adaptive Robust Large Volatility Matrix Estimation

Based on High-Frequency Financial Data*

Minseok Shin¹, Donggyu Kim¹ and Jianqing Fan²

¹KAIST and ²Princeton University

December 23, 2024

Abstract

Several novel statistical methods have been developed to estimate large integrated volatility matrices based on high-frequency financial data. To investigate their asymptotic behaviors, they require a sub-Gaussian or finite high-order moment assumption for observed log-returns, which cannot account for the heavy tail phenomenon of stock returns. Recently, a robust estimator was developed to handle heavy-tailed distributions with some bounded fourth-moment assumption. However, we often observe that log-returns have heavier tail distribution than the finite fourth-moment and that the degrees of heaviness of tails are heterogeneous over the asset and time period. In this paper, to deal with the heterogeneous heavy-tailed distributions, we develop an adaptive robust integrated volatility estimator that employs pre-averaging and truncation schemes based on jump-diffusion processes. We call this an adaptive robust pre-averaging realized volatility (ARP) estimator. We show that the ARP estimator

*Minseok Shin is a Ph.D. student, College of Business, KAIST, Seoul 02455, South Korea. Donggyu Kim is Ewon Assistant Professor, College of Business, KAIST, Seoul 02455, South Korea. His research was supported by KAIST Basic Research Funds by Faculty (A0601003029). Jianqing Fan is Frederick L. Moore'18 Professor of Finance, Department of Operations Research and Financial Engineering, Princeton University, Princeton, NJ 08544. His research was supported by NSFC grant No.71991471 and 71991470.

has a sub-Weibull tail concentration with only finite 2α -th moments for any $\alpha > 1$. In addition, we establish matching upper and lower bounds to show that the ARP estimation procedure is optimal. To estimate large integrated volatility matrices using the approximate factor model, the ARP estimator is further regularized using the principal orthogonal complement thresholding (POET) method. The numerical study is conducted to check the finite sample performance of the ARP estimator.

Key words: Heterogeneity, tail index, pre-averaging, minimax lower bound, optimality, POET, factor model.

1 Introduction

In modern financial studies and practices, volatility estimation is fundamental in risk management, performance evaluation, and portfolio allocation. Due to the wide availability of high-frequency financial data, many well-performing volatility estimation methods have been developed to estimate integrated volatilities. Examples include two-time scale realized volatility (TSRV) (Zhang et al., 2005), multi-scale realized volatility (MSRV) (Zhang, 2006, 2011), wavelet estimator (Fan and Wang, 2007), pre-averaging realized volatility (PRV) (Christensen et al., 2010; Jacod et al., 2009), kernel realized volatility (KRV) (Barndorff-Nielsen et al., 2008, 2011), quasi-maximum likelihood estimator (QMLE) (Aït-Sahalia et al., 2010; Xiu, 2010), and the local method of moments (Bibinger et al., 2014). One of the stylized features of financial data is the existence of price jumps, and the empirical studies have shown that the decomposition of daily variation into its continuous and jump components can better explain the volatility dynamics (Aït-Sahalia et al., 2012; Andersen et al., 2007; Barndorff-Nielsen and Shephard, 2006; Corsi et al., 2010; Song et al., 2020). For example, Fan and Wang (2007) and Zhang et al. (2016) employed wavelet method to identify the jumps given noisy high-frequency data. Mancini (2004) studied a threshold method for jump-detection and presented the order of an optimal threshold, and Davies and Tauchen (2018) further examined a data-driven type threshold method. These estimation methods perform well for a small number of assets. However, we often encounter a large number of

assets in practices such as portfolio allocation, which results in the curse of dimensionality. To overcome the curse of dimensionality and obtain an efficient and effective large volatility estimator, we often impose the approximate factor structure on the volatility matrix (Fan and Kim, 2018; Fan et al., 2013, 2018; Kim and Fan, 2019). For example, to account for common market factors such as sector, firm size, and book-to-market ratios, the factor-based high-dimensional Itô process is widely employed and the idiosyncratic volatility is assumed to be sparse (Aït-Sahalia and Xiu, 2017; Fan et al., 2016a,b; Kim et al., 2018; Kong, 2018). The principal orthogonal complement thresholding (POET) method (Fan et al., 2013) is often employed to estimate these low-rank plus sparse matrices.

The performance of the factor-based large volatility matrix estimator critically depends on the accuracy of each integrated volatility estimator. Specifically, sub-Weibull tail concentration for the input volatility matrix estimator is required to investigate its asymptotic behaviors. However, one stylized feature of stock return data is heavy-tailedness, which violates the sub-Gaussian assumption on the stock return data. Recently, with a bounded fourth-moment assumption on the microstructural noise, Fan and Kim (2018) developed a robust estimation method, which can attain sub-Gaussian tail concentration with the optimal convergence rate. See also Catoni (2012); Minsker (2018). However, the empirical studies have demonstrated that the bounded fourth-moment condition is often violated (Cont, 2001; Mao and Zhang, 2018; Massacci, 2017). Figure 1 shows the box plots of daily log kurtoses of the returns of the 200 most liquid assets in the S&P 500 index, calculated from 1-min log-return data with the previous tick scheme, for each of the 5 days in 2016: from the day with the largest interquartile range (IQR) to the day with the smallest IQR among 252 days. In Figure 1, we find that the log-return data are heavy-tailed and also have heterogeneous degrees of heaviness of tails over the different assets and different days. These facts generate the demand for developing an adaptive robust estimation method that can handle heterogeneous heavy-tailedness.

In this paper, we develop an adaptive robust integrated volatility estimator based on jump-diffusion processes contaminated by microstructural noises. We first use the pre-averaging scheme (Jacod et al., 2009) to adjust the unbalanced order relationship between

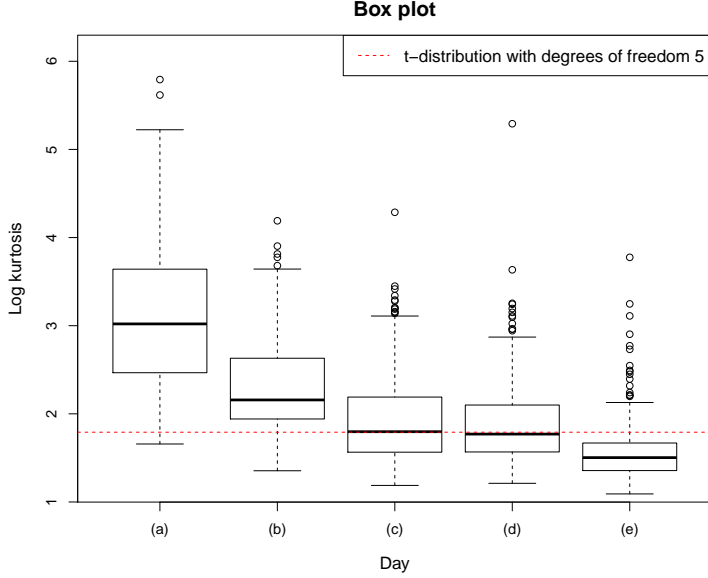


Figure 1: The box plots for the daily distributions of log kurtoses calculated from 1-min log returns based on the most liquid 200 stocks in S&P 500 index in 2016. Day (a) has the largest IQR, and days (b)–(e) have the 75th, 50th, 25th, and 0th (smallest) percentile of the IQR among 252 trading days in 2016, respectively. The red dash line marks the kurtosis for the t_5 -distribution.

the microstructural noises and true log-returns. We then employ the truncation method (Minsker, 2018) using the daily moment conditions of assets. Specifically, we truncate pre-averaged variables according to their heavy-tailedness, which allows for adaptive learning merits to be enjoyed. Also, the truncation method sufficiently mitigates the effect of the jump signal on the pre-averaged variables. We call the proposed estimator the adaptive robust pre-averaging realized volatility (ARP) estimator. We show that the ARP estimator has sub-Weibull tail concentration, with finite 2α -th moment assumption for any $\alpha > 1$. Also, by establishing matching upper and lower bounds for a pre-averaging estimator class, we show that the proposed estimator can achieve the optimal rate. To conduct inferences on large integrated volatility matrix using the ARP estimator, we assume the factor-based high-dimensional Itô process, which admits a low-rank plus sparse structure for the volatility matrix. The ARP estimator is further regularized by the principal orthogonal complement thresholding (POET) method, and we also investigate the theoretical properties of the POET

estimator from the ARP estimator.

The rest of the paper is organized as follows. Section 2 provides the model and data structure for estimating each daily integrated volatility, and Section 3 introduces an adaptive robust integrated volatility estimation method. Section 4 establishes the concentration property and optimality of the proposed estimator. In Section 5, with the approximate factor model, we show how to estimate the large integrated volatility matrix using the proposed estimation procedure. Section 6 conducts a simulation study to illustrate the finite sample performances of the proposed estimator and applies the estimation method to the S&P 500 stock. The conclusion is presented in Section 7, and proofs are collected in the Appendix.

2 The model set-up

We first define some notations. For any given p_1 by p_2 matrix $\mathbf{A} = (A_{ij})_{1 \leq i \leq p_1, 1 \leq j \leq p_2}$, let

$$\|\mathbf{A}\|_1 = \max_{1 \leq j \leq p_2} \sum_{i=1}^{p_1} |A_{ij}|, \quad \|\mathbf{A}\|_\infty = \max_{1 \leq i \leq p_1} \sum_{j=1}^{p_2} |A_{ij}|, \quad \|\mathbf{A}\|_{\max} = \max_{i,j} |A_{ij}|.$$

The matrix spectral norm $\|\mathbf{A}\|_2$ is the square root of the largest eigenvalue of $\mathbf{A}\mathbf{A}^\top$, and the Frobenius norm of \mathbf{A} is denoted by $\|\mathbf{A}\|_F = \sqrt{\text{tr}(\mathbf{A}^\top \mathbf{A})}$. We will use C to denote a generic positive constant whose value is free of n and p and may change from appearance to appearance.

Let $\mathbf{X}(t) = (X_1(t), \dots, X_p(t))^\top$ be the vector of true log-prices for p assets at time t . To model the high-frequency financial data, we often employ the jump-diffusion process as follows:

$$\begin{aligned} d\mathbf{X}(t) &= d\mathbf{X}^c(t) + \mathbf{L}(t)d\boldsymbol{\Lambda}(t) \\ &= \boldsymbol{\mu}(t)dt + \boldsymbol{\sigma}^\top(t)d\mathbf{W}_t + \mathbf{L}(t)d\boldsymbol{\Lambda}(t), \end{aligned} \tag{2.1}$$

where $\mathbf{X}^c(t) = (X_1^c(t), \dots, X_p^c(t))^\top$ with $\mathbf{X}^c(0) = \mathbf{X}(0)$ is the vector of true continuous log-prices at time t , $\boldsymbol{\mu}(t) = (\mu_1(t), \dots, \mu_p(t))^\top$ is a drift vector, $\boldsymbol{\sigma}(t)$ is a q by p matrix, \mathbf{W}_t

is a q dimensional independent Brownian motion, and the stochastic processes $\boldsymbol{\mu}(t)$, $\mathbf{X}(t)$, $\mathbf{X}^c(t)$, and $\boldsymbol{\sigma}(t)$ are defined on a filtered probability space $(\Omega, \mathcal{F}, \{\mathcal{F}_t, t \in [0, 1]\}, P)$ with filtration \mathcal{F}_t satisfying the usual conditions. For the jump part, $\mathbf{L}(t) = (L_1(t), \dots, L_p(t))^\top$ denotes the jump sizes and $\boldsymbol{\Lambda}(t) = (\Lambda_1(t), \dots, \Lambda_p(t))^\top$ is the p dimensional Poisson process with bounded intensity $\mathbf{I}(t) = (I_1(t), \dots, I_p(t))^\top$. The instantaneous volatility matrix of the continuous log-price $\mathbf{X}^c(t)$ is

$$\boldsymbol{\gamma}(t) = (\gamma_{ij}(t))_{1 \leq i, j \leq p} = \boldsymbol{\sigma}^\top(t) \boldsymbol{\sigma}(t),$$

and their quadratic variation is

$$\begin{aligned} [\mathbf{X}^c, \mathbf{X}^c]_t &= \int_0^t \boldsymbol{\gamma}(s) ds = \left(\int_0^t \gamma_{ij}(s) ds \right)_{1 \leq i, j \leq p} \\ &= \int_0^t \boldsymbol{\sigma}^\top(s) \boldsymbol{\sigma}(s) ds. \end{aligned}$$

The parameter of interest is the integrated volatility matrix of $\mathbf{X}^c(t)$,

$$\boldsymbol{\Gamma} = [\mathbf{X}^c, \mathbf{X}^c]_1 = \int_0^1 \boldsymbol{\gamma}(s) ds. \quad (2.2)$$

Unfortunately, we cannot observe the true log-prices $\mathbf{X}(t)$. In fact, observed high-frequency data are contaminated by microstructural noises. Furthermore, high-frequency data encounter a non-synchronization problem that transactions for multiple assets often arrive asynchronously. In this regard, we assume that the observed log-price $Y_i(t_{i,k})$ obeys the following model:

$$Y_i(t_{i,k}) = X_i(t_{i,k}) + \epsilon_i(t_{i,k}) \quad \text{for } i = 1, \dots, p, k = 0, \dots, n_i, \quad (2.3)$$

where $t_{i,k}$ is the k -th observation time point of the i -th asset, for fixed $i = 1, \dots, p$, $\epsilon_i(t_{i,k})$, $k = 0, \dots, n_i$, are i.i.d. noises with a mean of zero; and for $i, j = 1, \dots, p$, $\mathbb{E}[\epsilon_i(t) \epsilon_j(t)] = \eta_{ij}$ and $\epsilon_i(t)$ is independent of $\epsilon_j(t')$ for $t \neq t'$. In other words, we allow the microstructural noises to have cross-sectional dependency, and $\epsilon_i(\cdot)$ is independent of the price processes $X_i(\cdot)$.

To handle the microstructural noise issue, several estimation methods have been developed (Aït-Sahalia et al., 2010; Barndorff-Nielsen et al., 2008, 2011; Bibinger et al., 2014; Christensen et al., 2010; Fan and Wang, 2007; Jacod et al., 2009; Xiu, 2010; Zhang et al., 2005; Zhang, 2006, 2011). They work well for a finite number of assets and are widely adopted to develop large volatility matrix estimation procedures (Kim et al., 2016; Wang and Zou, 2010). However, the observed log-prices are heavy-tailed, so these methods cannot lead to the estimators with the sub-Weibull concentration bound that is essential asymptotic behaviors for large volatility matrix inferences. To tackle the heavy tail issue, Fan and Kim (2018) proposed the robust pre-averaging realized volatility estimation procedure, which can achieve the sub-Gaussian tail concentration with only finite fourth-moment condition on the microstructural noise. However, as shown in Figure 1, the degrees of heaviness of tails of log-returns of assets are heterogeneous across assets and over time. Furthermore, jumps in the true log-price process can also cause heavy-tailed distributions. To account for these features, we accommodate heterogeneous degrees of tail distributions based on the jump-diffusion process contaminated by microstructural noises. We assume that each asset has a different order of the highest finite absolute moment (see Assumption 1 in Section 4 for details).

3 Adaptive robust pre-averaging realized volatility estimator

In this section, we introduce an adaptive robust integrated volatility estimation procedure to handle the non-synchronization, price jump, and microstructural noise. To handle the non-synchronization problem, we consider the generalized sampling time proposed by Aït-Sahalia et al. (2010). We note that the generalized sampling time scheme includes other synchronization schemes such as previous tick (Zhang, 2011; Wang and Zou, 2010) and refresh time (Barndorff-Nielsen et al., 2011; Fan et al., 2012). See also Bibinger et al. (2014); Chen et al. (2020); Hayashi and Yoshida (2005, 2011); Malliavin et al. (2009); Park et al. (2016). We define the generalized sampling time as follows.

Definition 1. (Aït-Sahalia et al., 2010). A sequence of time points $\boldsymbol{\tau} = \{\tau_0, \dots, \tau_n\}$ is said to be the generalized sampling time if

- (1) $0 = \tau_0 < \tau_1 < \dots < \tau_{n-1} < \tau_n = 1$;
- (2) There exists at least one observation for each asset between consecutive τ_j 's;
- (3) The time intervals, $\{\Delta_j = \tau_j - \tau_{j-1}; j = 1, \dots, n\}$, satisfy $\sup_j \Delta_j \xrightarrow{p} 0$.

For the i -th asset, we select arbitrary observation, $Y_i(\tau_{i,k})$, between τ_{k-1} and τ_k . In other words, we choose any $\tau_{i,k} \in (\tau_{k-1}, \tau_k] \cap \{t_{i,l}, l = 0, 1, \dots, n_i\}$, $i = 1, \dots, p$.

Based on synchronized time, $\boldsymbol{\tau}$, we adopt the pre-averaging method to manage the microstructural noise (Jacod et al., 2009). For the observed log-returns, $Y_i(\tau_{i,k+1}) - Y_i(\tau_{i,k})$, $i = 1, \dots, p$, $k = 1, \dots, n-1$, the variance of the microstructural noise $2\eta_{ii}$ dominates the continuous log-return volatility $\int_{\tau_{i,k}}^{\tau_{i,k+1}} \gamma_{ii}(t) dt$. Therefore, it is hard to estimate the integrated volatility without smoothing to denoising. To adjust the order relationship between the noises and continuous log-returns, we use the following pre-averaged data to suppress the noises (Christensen et al., 2010; Jacod et al., 2009):

$$Z_i(\tau_k) = \sum_{l=0}^{K_n-1} g\left(\frac{l}{K_n}\right) \{Y_i(\tau_{i,k+l+1}) - Y_i(\tau_{i,k+l})\} \quad \text{for } i = 1, \dots, p, k = 1, \dots, n - K_n, \quad (3.1)$$

where the weight function $g(\cdot)$ is continuous and piecewise continuously differentiable with a piecewise Lipschitz derivative g' and satisfies $g(0) = g(1) = 0$ and $\int_0^1 \{g(t)\}^2 dt > 0$. In this paper, we choose bandwidth parameter K_n as $C_K n^{1/2}$ for some constants C_K , which provides the optimal rate $n^{-1/4}$. Then the continuous log-returns and noises in $Z_i(\tau_k)$'s are of the same order of magnitude (Fan and Kim, 2018). However, as shown in Figure 1, the pre-averaged random variables still have heterogeneous heavy tails across assets. Furthermore, there exist jump variations in the pre-averaged data. We note that in $Z_i(\tau_k)$, the jumps have higher order of magnitude than the noises and continuous log-returns. To handle these problems, we robustly estimate the volatility matrix by applying an adaptive truncation method according to the tails of the data.

Define the quadratic pre-averaged random variables

$$Q_{ij}(\tau_k) = \frac{n - K_n}{\phi K_n} Z_i(\tau_k) Z_j(\tau_k) \quad \text{for } i, j = 1, \dots, p, k = 1, \dots, n - K_n, \quad (3.2)$$

where $\phi = \frac{1}{K_n} \sum_{\ell=0}^{K_n-1} \left\{ g\left(\frac{\ell}{K_n}\right) \right\}^2$, and let

$$\alpha_{ij} = 2 \wedge \frac{2\alpha_i\alpha_j}{\alpha_i + \alpha_j}, \quad (3.3)$$

where α_i is the order of the highest finite moment for the continuous part of $Q_{ii}(\tau_k)$ (see Assumption 1 in Section 4). Then, to handle the heterogeneous heavy tails, we propose the following adaptive truncation method:

$$\widehat{T}_{ij,\theta}^\alpha = \frac{1}{(n - K_n)\theta_{ij}} \sum_{k=1}^{n - K_n} \psi_{\alpha_{ij}} \{ \theta_{ij} Q_{ij}(\tau_k) \}, \quad (3.4)$$

where θ_{ij} is a truncation parameter and $\psi_\alpha(x)$ is a bounded non-decreasing function defined for $1 < \alpha \leq 2$ as follows:

$$\psi_\alpha(x) = \begin{cases} -\log(1 - t_\alpha + c_\alpha t_\alpha^\alpha) & \text{if } x \geq t_\alpha \\ -\log(1 - x + c_\alpha x^\alpha) & \text{if } 0 \leq x \leq t_\alpha \\ \log(1 + x + c_\alpha |x|^\alpha) & \text{if } -t_\alpha \leq x \leq 0 \\ \log(1 - t_\alpha + c_\alpha t_\alpha^\alpha) & \text{if } x \leq -t_\alpha, \end{cases}$$

where $c_\alpha = \max \left\{ (\alpha - 1)/\alpha, \sqrt{(2 - \alpha)/\alpha} \right\}$ and $t_\alpha = (1/\alpha c_\alpha)^{1/(\alpha-1)}$. We note that the truncation detects the jumps and mitigates their impact on the estimator. Other truncation can also achieve similar goal (see Fan et al. (2021)). It will be shown that the proposed adaptive robust estimator $\widehat{T}_{ij,\theta}^\alpha$ possesses the sub-Weibull concentration bounds (see Theorem 1).

The adaptive robust estimator $\widehat{T}_{ij,\theta}^\alpha$ is, however, not a consistent estimator of the true integrated volatility Γ_{ij} since the noises still remain in each $Q_{ij}(\tau_k)$. Indeed, it will be shown

that $\widehat{T}_{ij,\theta}^\alpha$ converges to

$$T_{ij} = \Gamma_{ij} + \rho_{ij}, \quad (3.5)$$

where

$$\rho_{ij} = \frac{\sum_{k=1}^n \mathbf{1}(\tau_{i,k} = \tau_{j,k})}{\phi K_n} \zeta \eta_{ij}, \quad \zeta = \sum_{l=0}^{K_n-1} \left\{ g\left(\frac{l}{K_n}\right) - g\left(\frac{l+1}{K_n}\right) \right\}^2 = O\left(\frac{1}{K_n}\right),$$

with the covariance of noise η_{ij} defined in (2.3), and $\mathbf{1}(\cdot)$ is the indicator function. Hence, to estimate the integrated volatility Γ_{ij} , we adjust $\widehat{T}_{ij,\theta}^\alpha$ by subtracting an estimator of ρ_{ij} . For this purpose, let us first define an adaptive robust estimator, $\widehat{\rho}_{ij,\theta}^\alpha$, as

$$\widehat{\rho}_{ij,\theta}^\alpha = \frac{\zeta}{\phi K_n \theta_{\rho,ij}} \sum_{k=1}^{n-1} \psi_{\alpha_{ij}} \{ \theta_{\rho,ij} Q_{\rho,ij}(\tau_k) \}, \quad (3.6)$$

where

$$Q_{\rho,ij}(\tau_k) = \frac{1}{2} \{ Y_i(\tau_{i,k+1}) - Y_i(\tau_{i,k}) \} \{ Y_j(\tau_{j,k+1}) - Y_j(\tau_{j,k}) \} \quad (3.7)$$

for $i, j = 1, \dots, p$, $k = 1, \dots, n-1$, and $\theta_{\rho,ij}$ is truncation parameter that will be specified in Theorem 3. We now define the integrated volatility estimator as follows:

$$\widehat{\Gamma}_{ij} = \widehat{T}_{ij,\theta}^\alpha - \widehat{\rho}_{ij,\theta}^\alpha. \quad (3.8)$$

We call this the adaptive robust pre-averaging realized volatility (ARP) estimator. This provides a preliminary consistent estimate of $\widehat{\Gamma}_{ij}$, which will be further regularized.

4 Theoretical properties of the ARP estimator

In this section, we show the concentration property and optimality of the ARP estimator, by establishing matching upper and lower bounds for both $\widehat{T}_{ij,\theta}^\alpha$ and $\widehat{\rho}_{ij,\theta}^\alpha$. Note that we do not impose any restrictions on the jump sizes $\mathbf{L}(t)$ in (2.1). In other words, for the true log-prices, we only need assumptions for the continuous part. Specifically, Assumptions 1–2

are based on the following random variables,

$$\begin{aligned} Y_i^c(\tau_{i,k}) &= X_i^c(\tau_{i,k}) + \epsilon_i(\tau_{i,k}), \quad Z_i^c(\tau_k) = \sum_{l=0}^{K_n-1} g\left(\frac{l}{K_n}\right) \{Y_i^c(\tau_{i,k+l+1}) - Y_i^c(\tau_{i,k+l})\}, \\ Q_{ij}^c(\tau_k) &= \frac{n - K_n}{\phi K_n} Z_i^c(\tau_k) Z_j^c(\tau_k), \\ Q_{\rho,ij}^c(\tau_k) &= \frac{1}{2} \{Y_i^c(\tau_{i,k+1}) - Y_i^c(\tau_{i,k})\} \{Y_j^c(\tau_{j,k+1}) - Y_j^c(\tau_{j,k})\}, \end{aligned}$$

where $X_i^c(t)$ is the true continuous log-price process defined in (2.1) and the superscript c represents the continuous part of the true log-price. Now, to investigate asymptotic properties of $\widehat{T}_{ij,\theta}^\alpha$, we make the following assumptions.

Assumption 1.

(a) *There exist positive constants ν_μ and ν_γ such that*

$$\max_{1 \leq i \leq p} \max_{0 \leq t \leq 1} \mu_i(t) \leq \nu_\mu \text{ a.s. and } \max_{1 \leq i \leq p} \max_{0 \leq t \leq 1} \gamma_{ii}(t) \leq \nu_\gamma \text{ a.s.};$$

(b) *The generalized sampling time $\{\tau_j\}$ is independent of the price process $\mathbf{X}(t)$ and the noise $\epsilon_i(t_{i,k})$. The time intervals, $\{\Delta_j = \tau_j - \tau_{j-1}, 1 \leq j \leq n\}$, satisfy*

$$\max_{1 \leq j \leq n} \Delta_j \leq Cn^{-1} \text{ a.s.};$$

(c) *There exists a positive constant ν_Q such that*

$$\max_{1 \leq i \leq p} \mathbb{E} \{ |Q_{ii}^c(\tau_k)|^{\alpha_i} \} \leq \nu_Q$$

for all $1 \leq k \leq n - K_n$.

Remark 1. *For Assumption 1(a), the boundedness condition of the instantaneous volatility process $\gamma_{ii}(t)$ can be relaxed to the locally boundedness condition when we investigate the asymptotic behaviors of volatility estimators such as their convergence rate (see Aït-Sahalia and Xiu (2017)). Specifically, Lemma 4.4.9 in Jacod and Protter (2012) indicates that if the*

asymptotic result such as convergence in probability or stable convergence in law is satisfied under the boundedness condition, it is also satisfied under the locally boundedness condition. From this point of view, since we consider a finite time period, it is sufficient to investigate the asymptotic properties under the boundedness condition. Thus, Assumption 1(a) is not restrictive.

Remark 2. Assumption 1(c) is the finite moment condition, which entails that the quadratic pre-averaged variable, $Q_{ij}^c(\tau_k)$, for the continuous part satisfies

$$\mathbb{E} \left\{ |Q_{ij}^c(\tau_k)|^{\alpha_{ij}} \mid \mathcal{F}_{\tau_k} \right\} \leq U_{ij}(\tau_k) \text{ a.s.}$$

for all $1 \leq i, j \leq p$, $1 \leq k \leq n - K_n$, and some positive constants $U_{ij}(\tau_k)$, where α_{ij} is defined in (3.3) (see Proposition 2(a) in the Appendix). To account for the heterogeneous heavy-tailedness, we allow the tail index α_i to vary from 1 to infinity. If $\alpha_i = 2$ for all $i = 1, \dots, p$, it is the similar setting as that of Fan and Kim (2018), and the ARP estimator has universal truncation, which we call the universal robust pre-averaging realized volatility (URP) estimator. To investigate the heterogeneous heavy tail, we compare the ARP and URP estimators in the numerical study.

The theorem below shows that $\widehat{T}_{ij,\theta}^\alpha$ has the sub-Weibull tail concentration with a convergence rate of $n^{(1-\alpha_{ij})/2\alpha_{ij}}$.

Theorem 1. (Upper bound) Under the models (2.1) and (2.3) and Assumption 1, let $\delta^{-1} \in [n^c, e^{n^{1/2}}]$ for some positive constant $c > 0$. Take

$$\theta_{ij} = \left(\frac{K_n \log(3K_n^2 \delta^{-1})}{(\alpha_{ij} - 1) c_{\alpha_{ij}} S_{ij} (n - K_n)} \right)^{1/\alpha_{ij}},$$

where $S_{ij} = \frac{1}{n - K_n} \sum_{k=1}^{n - K_n} U_{ij}(\tau_k)$. Then we have, for sufficiently large n ,

$$\Pr \left\{ |\widehat{T}_{ij,\theta}^\alpha - T_{ij}| \leq C (n^{-1/2} \log \delta^{-1})^{(\alpha_{ij}-1)/\alpha_{ij}} \right\} \geq 1 - \delta. \quad (4.1)$$

Theorem 1 indicates that $\widehat{T}_{ij,\theta}^\alpha$ has a sub-Weibull concentration bound with a convergence

rate of $n^{(1-\alpha_{ij})/2\alpha_{ij}}$. Specifically, as long as $p^{b+2} \in [n^c, e^{n^{1/2}}]$ for some positive constant $c > 0$, we have

$$\Pr \left\{ \max_{1 \leq i, j \leq p} |\widehat{T}_{ij,\theta}^\alpha - T_{ij}| \geq C_b (n^{-1/2} \log p)^{(\alpha-1)/\alpha} \right\} \leq p^{-b}$$

for any constant $b > 0$ and $\alpha = \min_{1 \leq i \leq p} \alpha_i$, where C_b is some constant depending on b , which is the essential condition for investigating large matrix inferences (see Proposition 1). An interesting finding is that there is a trade-off between the convergence rate $n^{(1-\alpha_{ij})/2\alpha_{ij}}$ and the tail indexes α_i and α_j . This raises the question of whether the upper bound in (4.1) is optimal or not.

Let $\widehat{T}_{ij}(Q_{ij}(\tau_k), \delta) = \widehat{T}_{ij}(Q_{ij}(\tau_1), \dots, Q_{ij}(\tau_{n-K_n}), \delta)$ be any pre-averaging estimator for T_{ij} defined in (3.5), which takes values of pre-averaged variables $Q_{ij}(\tau_k), k = 1, \dots, n - K_n$, defined in (3.2). The following theorem establishes the lower bound for the maximum concentration probability among the class of pre-averaging estimators $\widehat{T}_{ij}(Q_{ij}(\tau_k), \delta)$ which satisfy $\max_{1 \leq i \leq p} \mathbb{E} \{ |Q_{ii}^c(\tau_k)|^{\alpha_i} \} \leq C$ for all $1 \leq k \leq n - K_n$.

Theorem 2. (Lower bound) *Under the assumptions in Theorem 1, let $\alpha_{ij} \in (1, 2)$ for some $1 \leq i, j \leq p$. Then we have, for sufficiently large n ,*

$$\min_{\widehat{T}_{ij}(Q_{ij}(\tau_k), \delta)} \max_{\mathbf{Q}^c \in \Xi(\alpha_1, \dots, \alpha_p)} \Pr \left\{ |\widehat{T}_{ij}(Q_{ij}(\tau_k), \delta) - T_{ij}| \geq C (n^{-1/2} \log \delta^{-1})^{(\alpha_{ij}-1)/\alpha_{ij}} \right\} \geq \delta, \quad (4.2)$$

where

$$\Xi(\alpha_1, \dots, \alpha_p) = \{ \mathbf{Q}^c = (Q_{ii}^c(\tau_k))_{i=1, \dots, p, k=1, \dots, n-K_n} : \max_{i,k} \mathbb{E} \{ |Q_{ii}^c(\tau_k)|^{\alpha_i} \} \leq C \}.$$

Theorem 2 shows that the lower bound is $n^{(1-\alpha_{ij})/2\alpha_{ij}}$, which matches the upper bound in Theorem 1. Thus, the proposed estimator obtains the optimal convergence rate of $n^{(1-\alpha_{ij})/2\alpha_{ij}}$.

Remark 3. *To handle the microstructural noise, we use the sub-sampling scheme, and the number of non-overlapping quadratic pre-averaged variables $Q_{ij}(\tau_k)$ is $Cn^{1/2}$, which is known as the optimal choice. That is, we are only able to use $n^{1/2}$ observations to estimate T_{ij} due to biases of varying spot volatilities, which is the cost of managing the microstructural*

noise. Thus, the optimal convergence rate is expected to be the square root of the rates of the estimators that are not affected by the microstructural noise. From this point of view, the convergence rate $n^{(1-\alpha_{ij})/2\alpha_{ij}}$ is consistent with the results in Devroye et al. (2016) and Sun et al. (2020).

Recall that the ARP estimator has the bias adjustment as follows:

$$\widehat{\Gamma}_{ij}^{\alpha} = \widehat{T}_{ij,\theta}^{\alpha} - \widehat{\rho}_{ij,\theta}^{\alpha}. \quad (4.3)$$

Thus, to establish the concentration inequality for the ARP estimator $\widehat{\Gamma}_{ij}^{\alpha}$, we need to investigate $\widehat{\rho}_{ij,\theta}^{\alpha}$. To do this, we use the quadratic log-return random variables $Q_{\rho,ij}(\tau_k)$ defined in (3.7) and need the following moment condition.

Assumption 2. *There exists a positive constant $\nu_{\rho,Q}$ such that*

$$\max_{1 \leq i \leq p} \mathbb{E} \left\{ \left| Q_{\rho,ii}^c(\tau_k) \right|^{\alpha_i} \right\} \leq \nu_{\rho,Q}$$

for all $1 \leq k \leq n-1$.

Remark 4. *Assumption 2 indicates that the continuous part of the observed log-return, $Y_i^c(\tau_{i,k+1}) - Y_i^c(\tau_{i,k})$, has finite $2\alpha_i$ -th moment. We note that Assumption 1(c) is satisfied under Assumption 1(a)–(b) and Assumption 2 (see Proposition 3 in the Appendix).*

Under Assumption 1(a)–(b) and Assumption 2, $Q_{\rho,ij}^c(\tau_k)$ has conditional α_{ij} -th moments,

$$\mathbb{E} \left\{ \left| Q_{\rho,ij}^c(\tau_k) \right|^{\alpha_{ij}} \middle| \mathcal{F}_{\tau_{k-1}} \right\} \leq U_{\rho,ij}(\tau_k) \text{ a.s.}$$

for all $1 \leq i, j \leq p$, $1 \leq k \leq n-1$, and some positive constants $U_{\rho,ij}(\tau_k)$ (see Proposition 2(b) in the Appendix). With this α_{ij} -th moment condition, we establish the concentration inequalities for the ARP estimator $\widehat{\Gamma}_{ij}^{\alpha}$ in the following theorem.

Theorem 3. *(Upper bound) Under the assumptions in Theorem 1 and Assumption 2, take*

$$\theta_{\rho,ij} = \left(\frac{\log(6\delta^{-1})}{(\alpha_{ij} - 1) c_{\alpha_{ij}} S_{\rho,ij}(n-1)} \right)^{1/\alpha_{ij}},$$

where $S_{\rho,ij} = \frac{1}{n-1} \sum_{k=1}^{n-1} U_{\rho,ij}(\tau_k)$. Then, for sufficiently large n , we have

$$\Pr \left\{ |\hat{\rho}_{ij,\theta}^\alpha - \rho_{ij}| \leq C (n^{-1} \log \delta^{-1})^{(\alpha_{ij}-1)/\alpha_{ij}} \right\} \geq 1 - \delta \quad (4.4)$$

and

$$\Pr \left\{ |\hat{\Gamma}_{ij}^\alpha - \Gamma_{ij}| \leq C (n^{-1/2} \log \delta^{-1})^{(\alpha_{ij}-1)/\alpha_{ij}} \right\} \geq 1 - 2\delta. \quad (4.5)$$

Theorem 3 shows that $\hat{\rho}_{ij,\theta}^\alpha$ has a sub-Weibull tail concentration bound with the convergence rate of $n^{(1-\alpha_{ij})/\alpha_{ij}}$, which is negligible compared to the upper bound in Theorem 1. Thus, the ARP estimator has a sub-Weibull tail concentration with the convergence rate of $n^{(1-\alpha_{ij})/2\alpha_{ij}}$ as in Theorem 1, which is optimal as shown in Theorems 1–2. Although the upper bound for $\hat{\rho}_{ij,\theta}^\alpha$ is dominated by the upper bound in Theorem 1, it is worth checking whether $\hat{\rho}_{ij,\theta}^\alpha$ is an optimal estimator or not. Let $\hat{\rho}_{ij}(Q_{\rho,ij}(\tau_k), \delta) = \hat{\rho}_{ij}(Q_{\rho,ij}(\tau_1), \dots, Q_{\rho,ij}(\tau_{n-1}), \delta)$ be any estimator for ρ_{ij} , possibly depending on δ . The following theorem provides a lower bound for the maximum concentration probability among the class of estimators $\hat{\rho}_{ij}(Q_{\rho,ij}(\tau_k), \delta)$ which satisfy $\max_{1 \leq i \leq p} \mathbb{E} \{ |Q_{\rho,ii}^c(\tau_k)|^{\alpha_i} \} \leq C$ for all $1 \leq k \leq n-1$.

Theorem 4. (Lower bound) Under the assumptions in Theorem 3, let $\alpha_{ij} \in (1, 2)$ for some $1 \leq i, j \leq p$. Then we have, for sufficiently large n ,

$$\min_{\hat{\rho}_{ij}(Q_{\rho,ij}(\tau_k), \delta)} \max_{\mathbf{Q}_\rho^c \in \Xi_\rho(\alpha_1, \dots, \alpha_p)} \Pr \left\{ |\hat{\rho}_{ij}(Q_{\rho,ij}(\tau_k), \delta) - \rho_{ij}| \geq C (\log \delta^{-1}/n)^{(\alpha_{ij}-1)/\alpha_{ij}} \right\} \geq \delta, \quad (4.6)$$

where

$$\Xi_\rho(\alpha_1, \dots, \alpha_p) = \{ \mathbf{Q}_\rho^c = (Q_{\rho,ii}^c(\tau_k))_{i=1, \dots, p, k=1, \dots, n-1} : \max_{i,k} \mathbb{E} \{ |Q_{\rho,ii}^c(\tau_k)|^{\alpha_i} \} \leq C \}.$$

The upper bound in (4.4) and lower bound in (4.6) match, which implies that $\hat{\rho}_{ij,\theta}^\alpha$ achieves the optimal rate. To sum up, the proposed estimators for T_{ij} and ρ_{ij} are both optimal in terms of convergence rate, which indicates that the ARP estimator is also optimal in the class of pre-averaging approaches.

5 Application to large volatility matrix estimation

In this section, we discuss how to estimate large integrated volatility matrices based on the approximate factor model using the ARP estimator. Specifically, we assume that the integrated volatility matrix has the following low-rank plus sparse structure:

$$\boldsymbol{\Gamma} = \sum_{k=1}^p \lambda_k \mathbf{q}_k \mathbf{q}_k^\top = \boldsymbol{\Theta} + \boldsymbol{\Sigma} = \sum_{k=1}^r \bar{\lambda}_k \bar{\mathbf{q}}_k \bar{\mathbf{q}}_k^\top + \boldsymbol{\Sigma},$$

where $\lambda_i > 0$ and $\bar{\lambda}_i > 0$ are the i -th largest eigenvalues of $\boldsymbol{\Gamma}$ and $\boldsymbol{\Theta}$, respectively, and their corresponding eigenvectors are \mathbf{q}_i and $\bar{\mathbf{q}}_i$. The low-rank volatility matrix $\boldsymbol{\Theta}$ accounts for the factor effect on the volatility matrix. We assume that the rank, r , of $\boldsymbol{\Theta}$ is bounded. The sparse volatility matrix $\boldsymbol{\Sigma}$ stands for idiosyncratic risk and satisfies the following sparse condition:

$$\max_{1 \leq i \leq p} \sum_{j=1}^p |\Sigma_{ij}|^q (\Sigma_{ii} \Sigma_{jj})^{(1-q)/2} \leq M_\sigma s_p \text{ a.s.}, \quad (5.1)$$

where M_σ is a positive random variable with $\text{E}(M_\sigma^2) < \infty$, $q \in [0, 1)$, and s_p is a deterministic function of p that grows slowly in p . When Σ_{ii} is bounded from below and $q = 0$, s_p measures the maximum number of nonvanishing elements in each row of matrix $\boldsymbol{\Sigma}$. This low-rank plus sparse structure is widely adopted for studying large matrix inferences (Aït-Sahalia and Xiu, 2017; Bai, 2003; Bai and Ng, 2002; Fan and Kim, 2018; Fan et al., 2018; Kim et al., 2018; Stock and Watson, 2002).

To harness the low-rank plus sparse structure, we employ the principal orthogonal complement thresholding (POET) method (Fan et al., 2013) as follows. We first decompose an input volatility matrix using the ARP estimators in (3.8) as follows:

$$\widehat{\boldsymbol{\Gamma}} = \left(\widehat{\Gamma}_{ij}^\alpha \right)_{i,j=1,\dots,p} = \sum_{k=1}^p \widehat{\lambda}_k \widehat{\mathbf{q}}_k \widehat{\mathbf{q}}_k^\top,$$

where $\widehat{\lambda}_i$ is the i -th largest eigenvalue of $\widehat{\boldsymbol{\Gamma}}$, and $\widehat{\mathbf{q}}_i$ is its corresponding eigenvector. Then, using the first r principal components, we estimate the low-rank factor volatility matrix $\boldsymbol{\Theta}$

as follows:

$$\widehat{\Theta} = \sum_{k=1}^r \widehat{\lambda}_k \widehat{\mathbf{q}}_k \widehat{\mathbf{q}}_k^\top.$$

To estimate the sparse volatility matrix Σ , we first calculate the input idiosyncratic volatility matrix estimator $\widetilde{\Sigma} = (\widetilde{\Sigma}_{ij})_{1 \leq i, j \leq p} = \widehat{\Gamma} - \widehat{\Theta}$ and employ the adapted thresholding method as follows:

$$\widehat{\Sigma}_{ij} = \begin{cases} \widetilde{\Sigma}_{ij} \vee 0, & \text{if } i = j \\ s_{ij}(\widetilde{\Sigma}_{ij}) \mathbf{1}(|\widetilde{\Sigma}_{ij}| \geq \varpi_{ij}), & \text{if } i \neq j \end{cases} \quad \text{and} \quad \widehat{\Sigma} = (\widehat{\Sigma}_{ij})_{1 \leq i, j \leq p},$$

where the thresholding function $s_{ij}(\cdot)$ satisfies that $|s_{ij}(x) - x| \leq \varpi_{ij}$, and the adaptive thresholding level $\varpi_{ij} = \varpi_n \sqrt{(\widetilde{\Sigma}_{ii} \vee 0)(\widetilde{\Sigma}_{jj} \vee 0)}$, which corresponds to the correlation thresholding at level ϖ_{ij} . Examples of the thresholding function $s_{ij}(x)$ include the soft thresholding function $s_{ij}(x) = x - \text{sign}(x)\varpi_{ij}$ and the hard thresholding function $s_{ij}(x) = x$. The tuning parameter ϖ_n will be specified in Proposition 1. In the empirical study, we use the hard thresholding method.

With the low-rank volatility matrix estimator $\widehat{\Theta} = (\widehat{\Theta}_{ij})_{1 \leq i, j \leq p}$ and the sparse volatility matrix estimator $\widehat{\Sigma} = (\widehat{\Sigma}_{ij})_{1 \leq i, j \leq p}$, we estimate the integrated volatility matrix Γ by

$$\widehat{\Gamma}_{POET} = \widehat{\Theta} + \widehat{\Sigma}.$$

To investigate asymptotic behaviors of the POET estimator, the sub-Weibull concentration inequality is required, and is satisfied by the ARP estimator as shown in Theorem 3. Thus, the POET estimator based on the ARP estimators can enjoy the similar asymptotic properties established in Fan and Kim (2018). To study its asymptotic behaviors, we need the following technical conditions imposed by Fan and Kim (2018), but the sub-Weibull concentration rate is different because we consider heterogeneous heavy-tailedness.

Assumption 3.

(a) Let $D_\lambda = \min\{\bar{\lambda}_i - \bar{\lambda}_{i+1} : 1 \leq i \leq r\}$, $(\lambda_1 + pM_\sigma)/D_\lambda \leq C_1$ a.s., and $D_\lambda \geq C_2 p$ a.s. for some generic constants C_1 and C_2 , where $\bar{\lambda}_{r+1} = 0$, M_σ is defined in (5.1), and $\bar{\lambda}_i$ and λ_i are the i -th eigenvalues of Θ and Γ , respectively;

(b) For some fixed constant C_3 , we have

$$\frac{p}{r} \max_{1 \leq i \leq p} \sum_{j=1}^r \bar{q}_{ij}^2 \leq C_3 \text{ a.s.},$$

where $\bar{\mathbf{q}}_j = (\bar{q}_{1j}, \dots, \bar{q}_{pj})^\top$ is the j -th eigenvector of Θ ;

(c) The smallest eigenvalue of Σ stays away from zero almost surely;

(d) $s_p/\sqrt{p} + (n^{-1/2} \log p)^{(\alpha-1)/\alpha} = o(1)$, where $\alpha = \min_{1 \leq i \leq p} \alpha_i$.

Under Assumption 3, we can establish the following proposition similar to the proof of Theorem 3 in Fan and Kim (2018). Below, we assume a generic input $\widehat{\Gamma}$ that satisfies (5.2). In particular, the ARP estimator satisfies the condition, as shown in Theorem 3.

Proposition 1. Under the model (2.1), let $\alpha = \min_{1 \leq i \leq p} \alpha_i$ and assume that the concentration inequality,

$$\Pr \left\{ \max_{1 \leq i, j \leq p} |\widehat{\Gamma}_{ij} - \Gamma_{ij}| \geq C (n^{-1/2} \log p)^{(\alpha-1)/\alpha} \right\} \leq p^{-1}, \quad (5.2)$$

Assumption 3, and the sparse condition (5.1) are met. Take $\varpi_n = C_\varpi \beta_n$ for some large fixed constant C_ϖ , where $\beta_n = M_\sigma s_p/p + (n^{-1/2} \log p)^{(\alpha-1)/\alpha}$. Then we have for sufficiently large n , with probability greater than $1 - 2p^{-1}$,

$$\|\widehat{\Sigma} - \Sigma\|_2 \leq CM_\sigma s_p \beta_n^{1-q}, \quad (5.3)$$

$$\|\widehat{\Sigma} - \Sigma\|_{\max} \leq C \beta_n, \quad (5.4)$$

$$\|\widehat{\Gamma}_{POET} - \Gamma\|_{\Gamma} \leq C \left[p^{1/2} (n^{-1/2} \log p)^{(2\alpha-2)/\alpha} + M_\sigma s_p \beta_n^{1-q} \right], \quad (5.5)$$

$$\|\widehat{\Gamma}_{POET} - \Gamma\|_{\max} \leq C \beta_n, \quad (5.6)$$

where the relative Frobenius norm $\|\mathbf{A}\|_{\Gamma}^2 = p^{-1} \|\Gamma^{-1/2} \mathbf{A} \Gamma^{-1/2}\|_F^2$. Furthermore, suppose that $M_\sigma s_p \beta_n^{1-q} = o(1)$. Then, with probability approaching 1, the minimum eigenvalue of $\widehat{\Sigma}$ is

bounded away from 0, $\widehat{\boldsymbol{\Gamma}}_{POET}$ is non-singular, and

$$\|\widehat{\boldsymbol{\Sigma}}^{-1} - \boldsymbol{\Sigma}^{-1}\|_2 \leq CM_\sigma s_p \beta_n^{1-q}, \quad (5.7)$$

$$\|\widehat{\boldsymbol{\Gamma}}_{POET}^{-1} - \boldsymbol{\Gamma}^{-1}\|_2 \leq CM_\sigma s_p \beta_n^{1-q}. \quad (5.8)$$

Remark 5. Unlike Theorem 3 in Fan and Kim (2018), Proposition 1 imposes the sub-Weibull concentration condition (5.2), which is the optimal rate with only finite 2α -th moments, as shown in Theorems 1–4. Note that if $2p^3 \in [n^c, e^{n^{1/2}}]$ for some positive constant $c > 0$, Theorem 3 shows that the ARP estimator satisfies (5.2) for $\delta = 1/(2p^3)$. Also, the POET estimator is consistent in terms of the relative Frobenius norm as long as $p = o(n^{(2\alpha-2)/\alpha})$. That is, the convergence rate is a function of the minimum tail index α .

5.1 Discussion on the tuning parameter selection

To implement the ARP estimation procedure, we need to choose tuning parameters. In this section, we discuss how to select the tuning parameters for the numerical studies.

We first estimate the tail index α_i as follows. Let $D_i(\tau_k) = Y_i(\tau_{i,k+1}) - Y_i(\tau_{i,k})$ for $k = 1, \dots, n-1$. Then the tail index is estimated by

$$\widehat{\alpha}_i = \min \left\{ a \in (1, c_{1\alpha}] \mid \frac{1}{n} \sum_{k=1}^n \left| \frac{D_i(\tau_k) - \bar{D}_i}{s_{D_i}} \right|^{2a} > c_{2\alpha} E |Z|^{2a} \right\}, \quad (5.9)$$

where \bar{D}_i and s_{D_i} are sample mean and sample standard deviation of $D_i(\tau_k)$, respectively, Z is a standard normal random variable, and $c_{1\alpha}$ and $c_{2\alpha}$ are two positive constants. If there is no a that satisfies above inequality, we choose $\widehat{\alpha}_i = c_{1\alpha}$. The intuition is that if the standardized $2a$ -th moment is too large, we would say that its $2a$ -th moment does not exist. To quantify the degree of largeness, we compare it with a multiple of corresponding standard Gaussian moment. That leads to the method in (5.9). In the empirical study, we use $c_{1\alpha} = 5$ and $c_{2\alpha} = 2$. Then the estimator, $\widehat{\alpha}_{ij}$, of α_{ij} is calculated as follows:

$$\widehat{\alpha}_{ij} = 2 \wedge \frac{2\widehat{\alpha}_i \widehat{\alpha}_j}{\widehat{\alpha}_i + \widehat{\alpha}_j}.$$

With $\widehat{\alpha}_{ij}$, we choose the thresholding level as follows:

$$\theta_{ij} = c \left(\frac{K_n \log p}{(\widehat{\alpha}_{ij} - 1) c_{\widehat{\alpha}_{ij}} \widehat{S}_{ij} (n - K_n)} \right)^{1/\widehat{\alpha}_{ij}} \quad (5.10)$$

and

$$\theta_{\rho,ij} = c \left(\frac{\log p}{(\widehat{\alpha}_{ij} - 1) c_{\widehat{\alpha}_{ij}} \widehat{S}_{\rho,ij} (n - 1)} \right)^{1/\widehat{\alpha}_{ij}}, \quad (5.11)$$

where $\widehat{S}_{ij} = \frac{1}{n - K_n} \sum_{k=1}^{n - K_n} \left\{ |Q_{ij}(\tau_k)|^{\widehat{\alpha}_{ij}} \right\}$, $\widehat{S}_{\rho,ij} = \frac{1}{n - 1} \sum_{k=1}^{n - 1} \left\{ |Q_{\rho,ij}(\tau_k)|^{\widehat{\alpha}_{ij}} \right\}$, and c is a tuning parameter. For the empirical study, we choose c as 0.15. Also, in the pre-averaging stage, we choose $K_n = \lfloor n^{1/2} \rfloor$ and $g(x) = x \wedge (1 - x)$.

Remark 6. *There are other ways to estimate the tail indices. For example, one of the most popular methods is Hill's estimator (Hill, 1975) which is consistent under some conditions. However, the performance of the Hill's estimator also heavily depends on the choice of the other tuning parameter. In fact, we conducted some empirical study using the Hill's estimator and found that the performance is not robust to the choice of the tuning parameter. That is, we run into the other tuning parameter choice problem. Furthermore, the result is not better than that of the proposed method in (5.9). Thus, we use the proposed method in the numerical study. To justify the proposed method, we need to investigate its asymptotic behavior. However, it may be a demanding task to develop some tuning parameter choice procedure that not only works well practically, but also has good properties in theory. We leave this for the future study.*

6 Numerical study

6.1 A simulation study

To check the finite sample performance of the ARP estimator, we conducted a simulation study. To obtain the low rank plus sparse structure, we considered the following true log-price

process,

$$d\mathbf{X}(t) = \boldsymbol{\mu}(t)dt + \boldsymbol{\vartheta}^\top(t)d\mathbf{W}_t^* + \boldsymbol{\sigma}^\top(t)d\mathbf{W}_t + \mathbf{L}(t)d\boldsymbol{\Lambda}(t),$$

where $\boldsymbol{\mu}(t) = (0.02, \dots, 0.02)^\top$, \mathbf{W}_t^* and \mathbf{W}_t are r and p dimensional independent Brownian motions, respectively, $\boldsymbol{\vartheta}(t)$ and $\boldsymbol{\sigma}(t)$ are r by r and p by p matrices, respectively, $\mathbf{L}(t)$ is jump sizes, and $\boldsymbol{\Lambda}(t)$ is the p dimensional Poisson process with the intensity $\mathbf{I}(t)$. We used a heterogeneous heavy tail process (heavy tail process 1), homogeneous heavy tail process (heavy tail process 2), and sub-Gaussian process to generate the volatility process. To generate two heavy tail processes, we used a setting similar to those in Wang and Zou (2010) and Fan and Kim (2018). Specifically, let $\boldsymbol{\sigma}(t)$ be the Cholesky decomposition of $\boldsymbol{\varsigma}(t) = (\varsigma_{ij}(t))_{1 \leq i, j \leq p}$. The diagonal elements of $\boldsymbol{\varsigma}(t)$ come from four different processes: geometric Ornstein-Uhlenbeck processes, the sum of two CIR processes (Cox et al., 1985; Barndorff-Nielsen, 2002), the volatility process in Nelson's GARCH diffusion limit model (Wang, 2002), and the two-factor log-linear stochastic volatility process (Huang and Tauchen, 2005) with leverage effect. Details can be found in Wang and Zou (2010). To control the tail behaviors of the instantaneous volatility matrix $\boldsymbol{\varsigma}(t)$, we used the t -distribution as follows:

$$\varsigma_{ii}(t_l) = (1 + |t_{df_i, l}|) \tilde{\varsigma}_{ii}(t_l),$$

where for $l = 1, \dots, n^{all}$, $t_{df_i, l}$ are the i.i.d. t -distributions with degrees of freedom df_i , $t_l = l/n^{all}$, and $\tilde{\varsigma}_{ii}(t_l)$ were generated by the above four different processes. To account for the heterogeneous heavy-tailed distribution (heavy tail process 1), df_i were generated from the $\text{unif}(2.5, 4)$, whereas for the homogeneous heavy-tailed distribution (heavy tail process 2), we set $df_i = 5$. To obtain the sparse instantaneous volatility matrix $\boldsymbol{\varsigma}(t)$, we generated its off-diagonal elements as follows:

$$\varsigma_{ij}(t_l) = \{\kappa(t_l)\}^{|i-j|} \sqrt{\varsigma_{ii}(t_l)\varsigma_{jj}(t_l)}, \quad 1 \leq i \neq j \leq p,$$

where the process $\kappa(t)$ is given by

$$\kappa(t) = \frac{e^{\frac{1}{2}u(t)} - 1}{e^{\frac{1}{2}u(t)} + 1}, \quad du(t) = 0.03\{0.64 - u(t)\}dt + 0.118u(t)dW_{\kappa,t},$$

$$W_{\kappa,t} = \sqrt{0.96}W_{\kappa,t}^0 - 0.2 \sum_{i=1}^p W_{it}/\sqrt{p},$$

and $W_{\kappa,t}^0, \kappa = 1, \dots, p$, are one-dimensional Brownian motions independent of the Brownian motions \mathbf{W}_t^* and \mathbf{W}_t . The low-rank instantaneous volatility matrix $\boldsymbol{\vartheta}^\top(t)\boldsymbol{\vartheta}(t)$ is $\mathbf{B}^\top\{\boldsymbol{\vartheta}^f(t)\}^\top\boldsymbol{\vartheta}^f(t)\mathbf{B}$, where $\mathbf{B} = (B_{ij})_{1 \leq i \leq r, 1 \leq j \leq p} \in \mathbb{R}^{r \times p}$ and B_{ij} was generated from the normal distribution with a mean of 0 and a standard deviation of 0.9, and $\boldsymbol{\vartheta}^f(t)$ was generated similar to $\boldsymbol{\sigma}(t)$. Specifically, $\boldsymbol{\vartheta}^f(t)$ is the Cholesky decomposition of $\boldsymbol{\varsigma}^f(t)$, and the diagonal elements of $\boldsymbol{\varsigma}^f(t)$ at time t_l were

$$\varsigma_{ii}^f(t_l) = \left\{ 1 + \left| t_{df_i,l}^f \right| \right\} \tilde{\varsigma}_{ii}^f(t_l),$$

where $t_{df_i,l}^f, l = 1, \dots, n^{all}$, are the i.i.d. t-distributions with degrees of freedom df_i , and $\tilde{\varsigma}_{ii}^f(t_l), l = 1, \dots, n^{all}$, were generated from the geometric Ornstein-Uhlenbeck processes. The off-diagonal elements of $\boldsymbol{\varsigma}^f(t)$ were set as zero. For the jump part, we chose $\mathbf{I}(t) = (5, \dots, 5)^\top$ and the jump size $L_i(t)$ was obtained from independent t-distribution with degrees of freedom df_i and standard deviation $0.2\sqrt{\int_0^1 \gamma_{ii}(t)dt}$. We also generated a sub-Gaussian process similar to the heavy tail process except that t-distribution terms were set as standard normal distribution terms.

To generate the observation time points, we first simulated $n^{all} - 1$ random variables independently from the $\text{unif}(0, 1)$. Then we took the order statistics of the $n^{all} - 1$ random variables as sampling time points $t_k, k = 1, \dots, n^{all} - 1$, with $t_0 = 0$ and $t_{n^{all}} = 1$. Based on these points, we generated non-synchronized data similar to the scheme in Aït-Sahalia et al. (2010) as follows. First, p random proportions $w_i, i = 1, \dots, p$, were independently generated from the $\text{unif}(0.8, 1)$. Second, we set each t_k as the observation time point of the i -th asset if and only if independent Bernoulli random variable with parameter w_i has a value of 1. Third, the noise-contaminated high-frequency observations $Y_i(t_{i,k})$ were generated from

the model (2.3). Specifically, the noise $\epsilon_i(t_{i,k})$ was obtained from independent t-distribution with degrees of freedom df_i and standard deviation $0.1\sqrt{\int_0^1 \gamma_{ii}(t)dt}$. We chose $p = 200$ and $r = 3$, and we varied n^{all} from 1000 to 4000. We employed the refresh time scheme to obtain synchronized data.

To investigate the effect of the adaptiveness of the proposed ARP procedure, we introduce a universal robust pre-averaging realized volatility (URP) estimator, which uses the same estimation procedure as the ARP estimator with $\hat{\alpha}_{ij} = 2$ for all $1 \leq i, j \leq p$. That is, the URP estimator truncates the pre-averaged variables with the universal tail index level. Thus, we calculated the input volatility matrix using the adaptive robust pre-averaging realized volatility matrix (ARPM), universal robust pre-averaging realized volatility matrix (URPM), and pre-averaging realized volatility matrix (PRVM) estimators. We used the tuning parameters discussed in Section 5.1 and set the tuning parameter c in (5.10)–(5.11) as 0.2. We note that, compared with the ARPM estimation procedure, the PRVM estimator was obtained by setting $\psi_\alpha(x) = x$ in Section 3 and the URPM estimator was obtained by setting $\alpha_{ij} = 2$ for all $i, j = 1, \dots, p$. This means that the PRVM estimator cannot account for the heavy tail and that the URPM estimator cannot explain the heterogeneity of different degrees of the heaviness of tail distributions.

To make the estimates positive semi-definite, we projected the volatility matrix estimators onto the positive semi-definite cone in the spectral norm. To calculate the POET estimators, we used the hard thresholding scheme and selected the thresholding level by minimizing the corresponding Frobenius norm. The average estimation errors under the Frobenius norm, relative Frobenius norm, $\|\cdot\|_\Gamma$, ℓ_2 -norm (spectral norm), and maximum norm were computed based on 1000 simulations. The average numbers of synchronized time points with the refresh time scheme were equal to 300.5, 600.4, 1199.7 for $n^{all} = 1000, 2000, 4000$, respectively.

Table 1: The mean squared errors (MSEs) of estimators for α_{ij} given $n^{all} = 1000, 2000, 4000$.

tail type \ n^{all}	MSE		
	1000	2000	4000
heterogeneous	0.136	0.100	0.064
homogeneous	0.001	0.001	0.001

Table 1 reports the mean squared errors (MSEs) of estimators for α_{ij} against the sample size n^{all} for two heavy-tail processes. For the heterogeneous heavy-tail process, $2\alpha_i$'s were generated from the $\text{unif}(2.5, 4)$ and $2\alpha_i=5$ for the homogeneous heavy-tail process. We calculated α_{ij} using (3.3). From Table 1, we can find that for the heterogeneous heavy-tail process, the MSE decreases as the sample size n^{all} increases. The MSEs for the homogeneous heavy-tail process are small regardless of n^{all} . We note that for the sub-Gaussian process, more than 99.99 percent of α_{ij} were estimated to be 2 (regarding as correctly estimated due to subGaussianity of the truncated average) for all n^{all} . These results indicate that the proposed tail index estimator works well.

Figure 2 plots the Frobenius, relative Frobenius, spectral, and max norm errors against the sample size n^{all} for the POET estimators from the ARPM, URPM, and PRVM estimators. Figure 3 depicts the spectral norm errors against the sample size n^{all} for the inverse POET estimators with the ARPM, URPM, and PRVM estimators. As expected, the ARPM estimator outperforms other estimators for the heterogeneous heavy-tail process. For the homogeneous heavy-tail and sub-Gaussian processes, the ARPM and URPM estimators both perform similarly and outperform the PRVM estimator. One possible explanation of the poor performance of the PRVM estimator in the Gaussian noise case is that the true return process contains heavy distributions over time and hence robust methods outperform. To sum up, the ARPM estimator is robust to the heterogeneity of the heaviness of tails and adapts to homogeneity of the heaviness of tails.

6.2 An empirical study

In this section, we applied the proposed ARP estimator to high-frequency trading data for 200 assets from January 1 to December 31, 2016 (252 trading days). The top 200 large trading volume stocks were selected from among the S&P 500, and the data was obtained from the Wharton Data Service (WRDS) system. Figure 4 plots the daily synchronized sample sizes from the refresh time scheme for 200 assets. As seen in Figure 4, sampling frequency higher than 1 minute can lead to the non-existence of the observation between some consecutive sample points. Hence, we employed 1-min log-return data with the previous tick scheme to

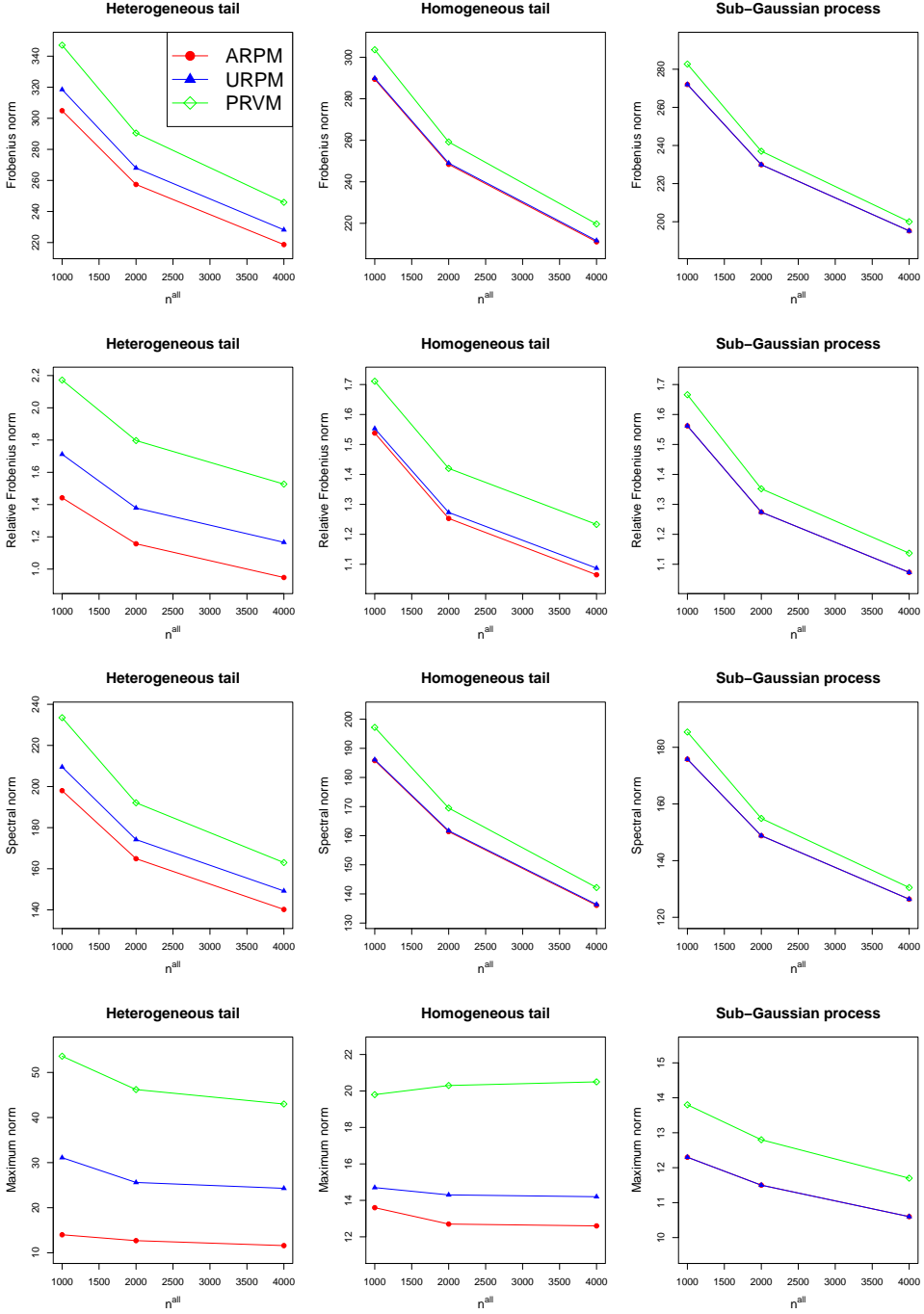


Figure 2: The Frobenius, relative Frobenius, spectral, and max norm error plots of the POET estimators with the ARPM, URPM, and PRVM estimators for $p = 200$ and $n^{all} = 1000, 2000, 4000$.

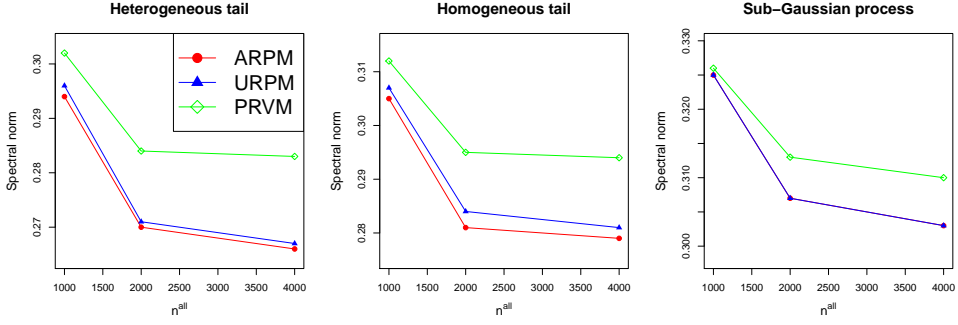


Figure 3: The spectral norm error plots of the inverse POET estimators with the ARPM, URPM, and PRVM estimators for $p = 200$ and $n^{all} = 1000, 2000, 4000$.

mitigate the potential heterogeneity from observed time intervals.

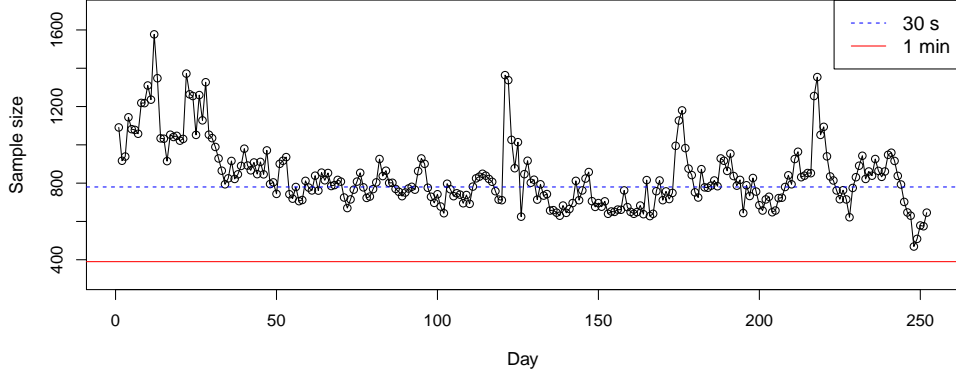


Figure 4: The number of daily synchronized samples from the refresh time scheme for 200 assets over 252 days in 2016. The blue dash and red solid lines mark the numbers of possible observations for 30-sec and 1-min log-returns in each trading day, which are 780 and 390 respectively.

To catch the heterogeneous heavy-tailedness over time, we estimated the tail indexes using the method (5.9) in Section 5.1. Figure 5 shows the box plots of daily estimated tail indexes $\hat{\alpha}_i$ of 200 assets for each of the 5 days in 2016: from the day with the largest IQR to the day with the smallest IQR among 252 days. Figure 5 shows that the tail indexes of observed log-returns are heterogeneous over time, which matches the daily kurtoses result in Figure 1. This supports the heterogeneous heavy tail assumption.

To apply POET estimation procedures, we first need to determine the rank r . We

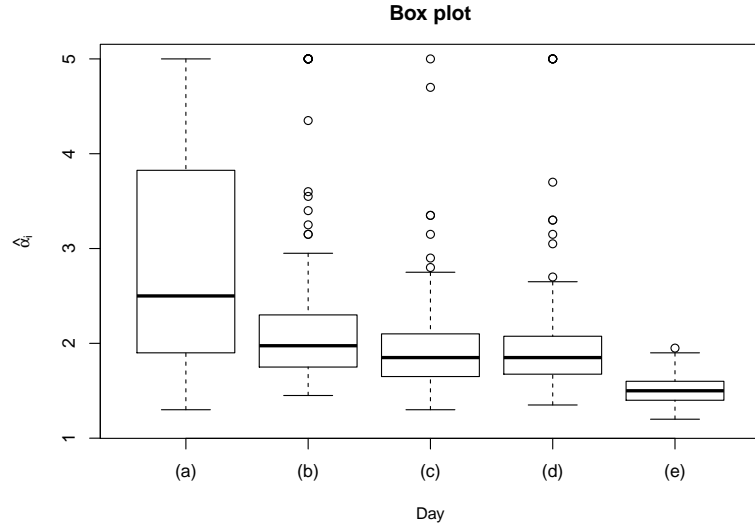


Figure 5: The box plots of the distributions of the daily estimated tail indexes $\hat{\alpha}_i$ for the 200 most liquid stocks among the S&P 500 index in 2016. Day (a) has the largest IQR, and days (b)–(e) have the 75th, 50th, 25th, and 0th (minimum) percentile of the IQR among 252 trading days in 2016, respectively.

calculated 252 daily integrated volatility matrices using the PRVM estimation procedure. Figure 6 shows the scree plot drawn using the eigenvalues from the sum of 252 PRVM estimates. As seen in Figure 6, the possible values of the rank r are 1, 2, 3, and hence we conducted the empirical study for $r = 1, 2, 3$.

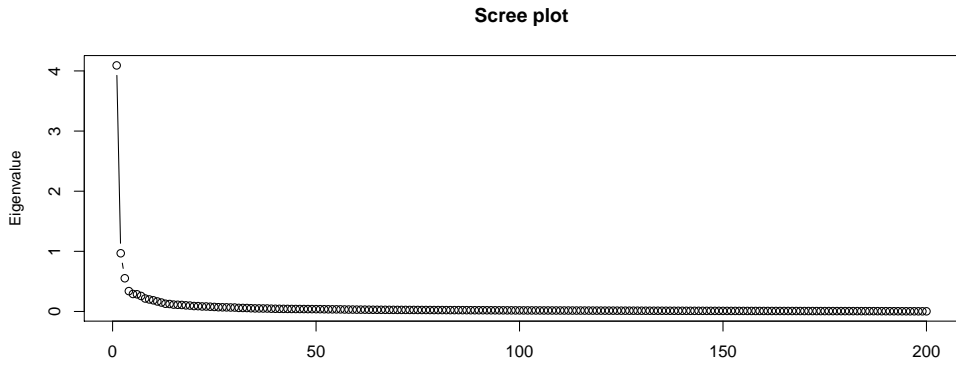


Figure 6: The scree plot of eigenvalues of the sum of 252 PRVM estimates.

To estimate the sparse volatility matrix Σ , we used the Global Industry Classification

Standard (GICS) (Fan et al., 2016a). Specifically, the covariance matrix for idiosyncratic components for the different sectors are set to zero and those for the same sector are maintained. This corresponds to hard-thresholding using the sector information. To make the estimates positive semi-definite, we projected the POET estimators onto the positive semi-definite cone in the spectral norm.

To check the performance of the proposed ARP estimation procedure, we first investigated the mean squared prediction error (MSPE) for the POET estimators, where the MSPE is defined as follows:

$$\text{MSPE}(\widehat{\boldsymbol{\Gamma}}) = \frac{1}{s-1} \sum_{d=1}^{s-1} \|\widehat{\boldsymbol{\Gamma}}_d - \widehat{\boldsymbol{\Gamma}}_{d+1}\|_F^2, \quad (6.1)$$

where s is the number of days in the period and $\widehat{\boldsymbol{\Gamma}}_d$ can be POET estimators from the ARPM, URPM, and PRVM estimators for the d -th day of the period. We used three different periods: 252 days, day 1 to day 126, and day 127 to day 252. Table 2 reports the MSPE results for the POET estimators from the inputs of the ARPM, URPM, and PRVM estimators. We find that for each period and rank r , the ARPM estimator has the smallest MSPE. The URPM estimator is slightly better than the PRVM estimator, but insignificantly so when compared with the ARPM estimator. One possible explanation is that the proposed ARP estimator can help deal with heterogeneous heavy-tailed distributions when estimating integrated volatility matrices.

To check the out-of-sample performance, we applied the ARPM, URPM, and PRVM estimators to the following minimum variance portfolio allocation problem:

$$\min_{\omega} \omega^\top \widehat{\boldsymbol{\Gamma}} \omega, \quad \text{subject to } \omega^\top \mathbf{J} = 1 \text{ and } \|\omega\|_1 \leq c_0,$$

where $\mathbf{J} = (1, \dots, 1)^\top \in \mathbb{R}^p$, the gross exposure constraint c_0 was changed from 1 to 6, and $\widehat{\boldsymbol{\Gamma}}$ could be the POET estimators from the ARPM, URPM, and PRVM estimators. To calculate the out-of-sample risks, we constructed the portfolios at the beginning of each trading day using the stock weights calculated using the data from the previous day. We then held this for one day and calculated the square root of realized volatility using the 10-min portfolio log-returns. Their average was used for out-of-sample risk. We tested the performances for

Table 2: The MSPEs of the POET estimators from the ARPM, URPM, and PRVM estimators (period 1: 252 days, period 2: day 1 to day 126, period 3: day 127 to day 252).

		MSPE $\times 10^4$		
		Rank r		
		1	2	3
Period 1	ARPM	4.8564	5.1218	5.1113
	URPM	10.1265	10.3767	10.3925
	PRVM	11.4088	11.7067	11.7266
Period 2	ARPM	8.8156	9.2538	9.2013
	URPM	19.0892	19.4768	19.4659
	PRVM	21.5247	21.9896	21.9807
Period 3	ARPM	0.9240	1.0181	1.0493
	URPM	1.2305	1.3443	1.3872
	PRVM	1.3683	1.5004	1.5496

three different periods: 252 days, day 1 to day 126, and day 127 to day 252.

Figure 7 depicts the out-of-sample risks of the portfolios constructed by the POET estimators from the ARPM, URPM, and PRVM estimators. We can find that, for the purpose of portfolio allocation, the ARPM estimator shows a stable result and has the smallest risks. The URPM estimator performs better than the PRVM estimator, but the improvement is less compared to that of the ARPM estimator. It is worth noting that the results do not significantly depend on the period and rank r . These results lend further support to our claim that the heavy-tailed distributions of observed log-returns are heterogeneous, as shown in Figure 1 and Figure 5, and the proposed ARP estimation procedure can account for the heterogeneity of the degrees of heaviness of tail distributions.

7 Conclusion

In this paper, we develop the adaptive robust pre-averaging realized volatility (ARP) estimation method to handle the heterogeneous heavy-tailed distributions of stock returns. To account for the heterogeneity of the heavy-tailedness from microstructural noises and price jumps, the ARP estimator truncates quadratic pre-averaged random variables according to daily tail indices. We show that the proposed ARP estimator achieves sub-Weibull tail con-

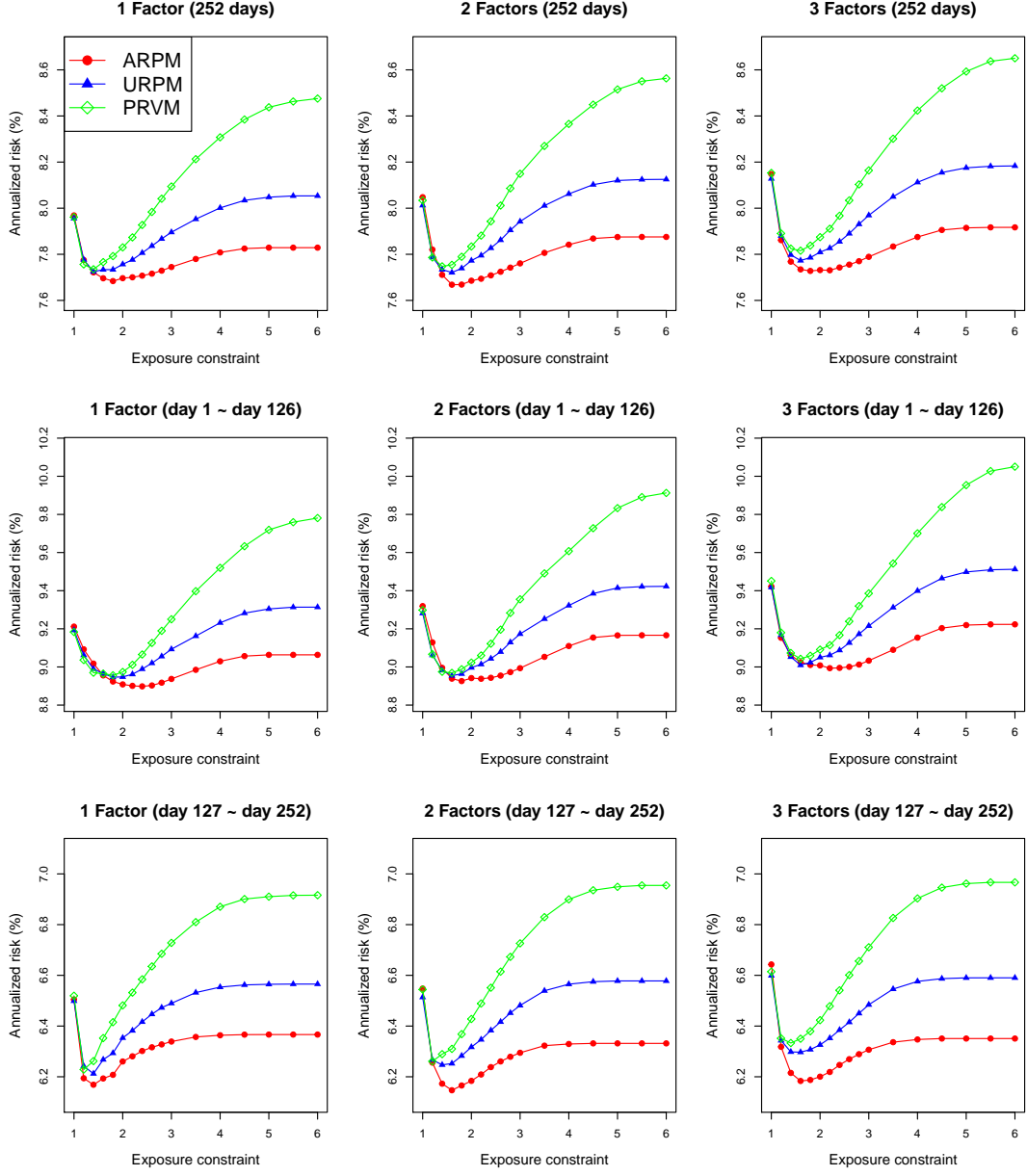


Figure 7: The out-of-sample risks of the optimal portfolios constructed by using the POET estimators from the ARPM, URPM, and PRVM estimators.

centration with the optimal convergence rate by showing that its upper bound is matched with its lower bound. To estimate large integrated volatility matrices, the ARP estimator is further regularized using the POET procedure, and the asymptotic properties of the POET estimator from the ARP estimator are also investigated. In the empirical study, for the

purpose of portfolio allocation, the POET estimator based on the ARP estimator performs the best. These findings suggest that when it comes to estimating the integrated volatility matrices, the proposed ARP estimation procedure helps handle the heterogeneous tail distributions of observed log-returns.

The non-synchronization could be other source of the heavy-tailness and also the heterogeneity of time intervals can cause some heterogeneous variation. However, in this paper, we do not focus on this issue and mainly consider the noise and jump as the source of the heavy-tailness. It would be interesting and important to study the observation time point in the aspect of the heavy-tailness. Furthermore, there are other possible sources of the heavy-tailness and it is important to know what actually causes heavy-tailness. We leave these interesting questions for the future study.

References

Aït-Sahalia, Y., Fan, J., and Xiu, D. (2010). High-frequency covariance estimates with noisy and asynchronous financial data. *Journal of the American Statistical Association*, 105(492):1504–1517.

Aït-Sahalia, Y., Jacod, J., and Li, J. (2012). Testing for jumps in noisy high frequency data. *Journal of Econometrics*, 168(2):207–222.

Aït-Sahalia, Y. and Xiu, D. (2017). Using principal component analysis to estimate a high dimensional factor model with high-frequency data. *Journal of Econometrics*, 201(2):384–399.

Andersen, T. G., Bollerslev, T., and Diebold, F. X. (2007). Roughing it up: Including jump components in the measurement, modeling, and forecasting of return volatility. *The review of economics and statistics*, 89(4):701–720.

Bai, J. (2003). Inferential theory for factor models of large dimensions. *Econometrica*, 71(1):135–171.

Bai, J. and Ng, S. (2002). Determining the number of factors in approximate factor models. *Econometrica*, 70(1):191–221.

Barndorff-Nielsen, O. E. (2002). Econometric analysis of realized volatility and its use in estimating stochastic volatility models. *Journal of the Royal Statistical Society: Series B (Statistical Methodology)*, 64(2):253–280.

Barndorff-Nielsen, O. E., Hansen, P. R., Lunde, A., and Shephard, N. (2008). Designing realized kernels to measure the ex post variation of equity prices in the presence of noise. *Econometrica*, 76(6):1481–1536.

Barndorff-Nielsen, O. E., Hansen, P. R., Lunde, A., and Shephard, N. (2011). Multivariate realised kernels: consistent positive semi-definite estimators of the covariation of equity prices with noise and non-synchronous trading. *Journal of Econometrics*, 162(2):149–169.

Barndorff-Nielsen, O. E. and Shephard, N. (2006). Econometrics of testing for jumps in financial economics using bipower variation. *Journal of financial Econometrics*, 4(1):1–30.

Bibinger, M., Hautsch, N., Malec, P., and Reiß, M. (2014). Estimating the quadratic co-variation matrix from noisy observations: Local method of moments and efficiency. *The Annals of Statistics*, 42(4):1312–1346.

Catoni, O. (2012). Challenging the empirical mean and empirical variance: a deviation study. *Annales de l’Institut Henri Poincaré, Probabilités et Statistiques*, 48(4):1148–1185.

Chen, D., Mykland, P. A., and Zhang, L. (2020). The five trolls under the bridge: Principal component analysis with asynchronous and noisy high frequency data. *Journal of the American Statistical Association*, 115(532):1960–1977.

Christensen, K., Kinnebrock, S., and Podolskij, M. (2010). Pre-averaging estimators of the ex-post covariance matrix in noisy diffusion models with non-synchronous data. *Journal of Econometrics*, 159(1):116–133.

Cont, R. (2001). Empirical properties of asset returns: stylized facts and statistical issues. *Quantitative Finance*, 1(2):223–236.

Corsi, F., Pirino, D., and Reno, R. (2010). Threshold bipower variation and the impact of jumps on volatility forecasting. *Journal of Econometrics*, 159(2):276–288.

Cox, J. C., Ingersoll Jr, J. E., and Ross, S. A. (1985). A theory of the term structure of interest rates. *Econometrica: Journal of the Econometric Society*, 53:385–407.

Davies, R. and Tauchen, G. (2018). Data-driven jump detection thresholds for application in jump regressions. *Econometrics*, 6(2):16.

Devroye, L., Lerasle, M., Lugosi, G., and Oliveira, R. I. (2016). Sub-gaussian mean estimators. *The Annals of Statistics*, 44(6):2695–2725.

Fan, J., Furger, A., and Xiu, D. (2016a). Incorporating global industrial classification standard into portfolio allocation: A simple factor-based large covariance matrix estimator with high-frequency data. *Journal of Business & Economic Statistics*, 34(4):489–503.

Fan, J. and Kim, D. (2018). Robust high-dimensional volatility matrix estimation for high-frequency factor model. *Journal of the American Statistical Association*, 113(523):1268–1283.

Fan, J., Li, Y., and Yu, K. (2012). Vast volatility matrix estimation using high-frequency data for portfolio selection. *Journal of the American Statistical Association*, 107(497):412–428.

Fan, J., Liao, Y., and Liu, H. (2016b). An overview of the estimation of large covariance and precision matrices. *The Econometrics Journal*, 19(1):C1–C32.

Fan, J., Liao, Y., and Mincheva, M. (2013). Large covariance estimation by thresholding principal orthogonal complements. *Journal of the Royal Statistical Society: Series B (Statistical Methodology)*, 75(4):603–680.

Fan, J., Wang, W., and Zhong, Y. (2018). An ℓ_∞ eigenvector perturbation bound and its application to robust covariance estimation. *Journal of Machine Learning Research*, 18(207):1–42.

Fan, J., Wang, W., and Zhu, Z. (2021). A shrinkage principle for heavy-tailed data: High-dimensional robust low-rank matrix recovery. *Annals of Statistics*, page to appear.

Fan, J. and Wang, Y. (2007). Multi-scale jump and volatility analysis for high-frequency financial data. *Journal of the American Statistical Association*, 102(480):1349–1362.

Hayashi, T. and Yoshida, N. (2005). On covariance estimation of non-synchronously observed diffusion processes. *Bernoulli*, 11(2):359–379.

Hayashi, T. and Yoshida, N. (2011). Nonsynchronous covariation process and limit theorems. *Stochastic processes and their applications*, 121(10):2416–2454.

Hill, B. M. (1975). A simple general approach to inference about the tail of a distribution. *The annals of statistics*, pages 1163–1174.

Huang, X. and Tauchen, G. (2005). The relative contribution of jumps to total price variance. *Journal of financial econometrics*, 3(4):456–499.

Jacod, J., Li, Y., Mykland, P. A., Podolskij, M., and Vetter, M. (2009). Microstructure noise in the continuous case: the pre-averaging approach. *Stochastic processes and their applications*, 119(7):2249–2276.

Jacod, J. and Protter, P. (2012). *Discretization of Processes*. Springer.

Kim, D. and Fan, J. (2019). Factor garch- \hat{I} ô models for high-frequency data with application to large volatility matrix prediction. *Journal of Econometrics*, 208(2):395–417.

Kim, D., Liu, Y., and Wang, Y. (2018). Large volatility matrix estimation with factor-based diffusion model for high-frequency financial data. *Bernoulli*, 24(4B):3657–3682.

Kim, D., Wang, Y., and Zou, J. (2016). Asymptotic theory for large volatility matrix estimation based on high-frequency financial data. *Stochastic Processes and their Applications*, 126:3527—3577.

Kong, X.-B. (2018). On the systematic and idiosyncratic volatility with large panel high-frequency data. *Annals of Statistics*, 46(3):1077–1108.

Malliavin, P., Mancino, M. E., et al. (2009). A fourier transform method for nonparametric estimation of multivariate volatility. *The Annals of Statistics*, 37(4):1983–2010.

Mancini, C. (2004). Estimation of the characteristics of the jumps of a general poisson-diffusion model. *Scandinavian Actuarial Journal*, 2004(1):42–52.

Mao, G. and Zhang, Z. (2018). Stochastic tail index model for high frequency financial data with bayesian analysis. *Journal of Econometrics*, 205(2):470–487.

Massacci, D. (2017). Tail risk dynamics in stock returns: Links to the macroeconomy and global markets connectedness. *Management Science*, 63(9):3072–3089.

Minsker, S. (2018). Sub-gaussian estimators of the mean of a random matrix with heavy-tailed entries. *The Annals of Statistics*, 46(6A):2871–2903.

Park, S., Hong, S. Y., and Linton, O. (2016). Estimating the quadratic covariation matrix for asynchronously observed high frequency stock returns corrupted by additive measurement error. *Journal of Econometrics*, 191(2):325–347.

Song, X., Kim, D., Yuan, H., Cui, X., Lu, Z., Zhou, Y., and Wang, Y. (2020). Volatility analysis with realized garch-itô models. *Journal of Econometrics*.

Stock, J. H. and Watson, M. W. (2002). Forecasting using principal components from a large number of predictors. *Journal of the American statistical association*, 97(460):1167–1179.

Sun, Q., Zhou, W.-X., and Fan, J. (2020). Adaptive huber regression. *Journal of the American Statistical Association*, 115(529):254–265.

Wang, Y. (2002). Asymptotic nonequivalence of garch models and diffusions. *The Annals of Statistics*, 30(3):754–783.

Wang, Y. and Zou, J. (2010). Vast volatility matrix estimation for high-frequency financial data. *The Annals of Statistics*, 38(2):943–978.

Xiu, D. (2010). Quasi-maximum likelihood estimation of volatility with high frequency data. *Journal of Econometrics*, 159(1):235–250.

Zhang, L. (2006). Efficient estimation of stochastic volatility using noisy observations: A multi-scale approach. *Bernoulli*, 12(6):1019–1043.

Zhang, L. (2011). Estimating covariation: Epps effect, microstructure noise. *Journal of Econometrics*, 160(1):33–47.

Zhang, L., Mykland, P. A., and Aït-Sahalia, Y. (2005). A tale of two time scales: Determining integrated volatility with noisy high-frequency data. *Journal of the American Statistical Association*, 100(472):1394–1411.

Zhang, X., Kim, D., and Wang, Y. (2016). Jump variation estimation with noisy high frequency financial data via wavelets. *Econometrics*, 4(3):34.

A Appendix

A.1 Proof of Theorem 1

For simplicity, we denote K_n by K . Let

$$\begin{aligned}
\bar{X}_i(\tau_k) &= \sqrt{\frac{n-K}{\phi K}} \sum_{l=0}^{K-1} g\left(\frac{l}{K}\right) \{X_i^c(\tau_{i,k+l+1}) - X_i^c(\tau_{i,k+l})\} \\
&= \sqrt{\frac{n-K}{\phi K}} \sum_{l=0}^{K-1} g\left(\frac{l}{K}\right) \int_{\tau_{i,k+l}}^{\tau_{i,k+l+1}} \mu_i(t) dt \\
&\quad + \sqrt{\frac{n-K}{\phi K}} \sum_{l=0}^{K-1} g\left(\frac{l}{K}\right) \int_{\tau_{i,k+l}}^{\tau_{i,k+l+1}} e_i^\top \boldsymbol{\sigma}^\top(t) d\mathbf{W}_t \\
&= \bar{X}_i^\mu(\tau_k) + \bar{X}_i^\sigma(\tau_k),
\end{aligned}$$

where e_i is the $p \times 1$ vector with all 0s except for a 1 in the i -th coordinate and

$$\begin{aligned}
\bar{\epsilon}_i(\tau_k) &= \sqrt{\frac{n-K}{\phi K}} \sum_{l=0}^{K-1} g\left(\frac{l}{K}\right) \{\epsilon_i(\tau_{i,k+l+1}) - \epsilon_i(\tau_{i,k+l})\} \\
&= \sqrt{\frac{n-K}{\phi K}} \sum_{l=0}^{K-1} \left\{ g\left(\frac{l}{K}\right) - g\left(\frac{l+1}{K}\right) \right\} \epsilon_i(\tau_{i,k+l+1}).
\end{aligned}$$

Then we have

$$Q_{ij}^c(\tau_k) = [\bar{X}_i(\tau_k) + \bar{\epsilon}_i(\tau_k)] [\bar{X}_j(\tau_k) + \bar{\epsilon}_j(\tau_k)]. \quad (\text{A.1})$$

Proposition 2. *Under models (2.1) and (2.3), (a) and (b) hold for all $1 \leq i, j \leq p$ and sufficiently large n .*

(a) *Under Assumption 1, there exist positive constants $U_{ij}(\tau_k)$ whose values are free of n and p such that*

$$E \left\{ |Q_{ij}^c(\tau_k)|^{\alpha_{ij}} \mid \mathcal{F}_{\tau_k} \right\} \leq U_{ij}(\tau_k) \text{ a.s.}$$

for all $1 \leq k \leq n - K_n$.

(b) *Under Assumption 1(a)–(b) and Assumption 2, there exist positive constants $U_{\rho,ij}(\tau_k)$*

whose values are free of n and p such that

$$\mathbb{E} \left\{ \left| Q_{\rho,ij}^c(\tau_k) \right|^{\alpha_{ij}} \middle| \mathcal{F}_{\tau_{k-1}} \right\} \leq U_{\rho,ij}(\tau_k) \text{ a.s.}$$

for all $1 \leq k \leq n-1$.

Proof of Proposition 2. First, consider (a). By the Hölder's inequality,

$$\begin{aligned} & \mathbb{E} \left[\left| Q_{ij}^c(\tau_k) \right|^{2\alpha_i \alpha_j / (\alpha_i + \alpha_j)} \middle| \mathcal{F}_{\tau_k} \right] \\ & \leq \left\{ \mathbb{E} \left[\left| Q_{ii}^c(\tau_k) \right|^{\alpha_i} \middle| \mathcal{F}_{\tau_k} \right] \right\}^{\alpha_j / (\alpha_i + \alpha_j)} \left\{ \mathbb{E} \left[\left| Q_{jj}^c(\tau_k) \right|^{\alpha_j} \middle| \mathcal{F}_{\tau_k} \right] \right\}^{\alpha_i / (\alpha_i + \alpha_j)} \text{ a.s.} \end{aligned}$$

Therefore, it suffices to show that

$$\mathbb{E} \left[\left| Q_{ii}^c(\tau_k) \right|^{\alpha_i} \middle| \mathcal{F}_{\tau_k} \right] \leq C \text{ a.s.}$$

By Assumption 1(c) and (A.1), we have

$$\begin{aligned} \nu_Q & \geq \mathbb{E} \left[\left| Q_{ii}^c(\tau_k) \right|^{\alpha_i} \right] \\ & = \mathbb{E} \left[\left| \bar{X}_i(\tau_k) + \bar{\epsilon}_i(\tau_k) \right|^{2\alpha_i} \right] \\ & = \mathbb{E} \left\{ \mathbb{E} \left[\left| \bar{X}_i(\tau_k) + \bar{\epsilon}_i(\tau_k) \right|^{2\alpha_i} \middle| \bar{\epsilon}_i(\tau_k) \right] \right\} \\ & \geq \mathbb{E} \left\{ \left| \mathbb{E} \left[\bar{X}_i(\tau_k) + \bar{\epsilon}_i(\tau_k) \middle| \bar{\epsilon}_i(\tau_k) \right] \right|^{2\alpha_i} \right\} \\ & \geq \mathbb{E} \left\{ \left| \left| \bar{\epsilon}_i(\tau_k) \right| - \left| \mathbb{E} \left[\bar{X}_i(\tau_k) \right] \right| \right|^{2\alpha_i} \right\}. \end{aligned}$$

Also, by the fact that $|\bar{X}_i^\mu(\tau_k)| \leq Cn^{-1/4}$ a.s., we have

$$\left| \mathbb{E} \left[\bar{X}_i(\tau_k) \right] \right| = \left| \mathbb{E} \left[\bar{X}_i^\mu(\tau_k) \right] \right| \leq Cn^{-1/4} \text{ a.s.}$$

Hence, using the Hölder's inequality, we can show

$$\mathbb{E} \left[\left| \bar{\epsilon}_i(\tau_k) \right|^{2\alpha_i} \right] \leq C.$$

Then, by the Lipschitz continuity of $g(\cdot)$, we have

$$\begin{aligned}
\mathbb{E} \left[|Q_{ii}^c(\tau_k)|^{\alpha_i} \middle| \mathcal{F}_{\tau_k} \right] &= \mathbb{E} \left[|\bar{X}_i^\mu(\tau_k) + \bar{X}_i^\sigma(\tau_k) + \bar{\epsilon}_i(\tau_k)|^{2\alpha_i} \middle| \mathcal{F}_{\tau_k} \right] \\
&\leq C + C \mathbb{E} \left[|\bar{X}_i^\sigma(\tau_k)|^{2\alpha_i} \middle| \mathcal{F}_{\tau_k} \right] \\
&\leq C + C \left| \frac{n-K}{\phi K} \sum_{l=0}^{K-1} g^2 \left(\frac{l}{K} \right) \frac{\nu_\gamma}{n} \right|^{\alpha_i} \\
&\leq C \text{ a.s.},
\end{aligned} \tag{A.2}$$

where the first inequality is due to the Hölder's inequality and the second inequality is from the Burkholder-Davis-Gundy inequality. Then (a) is proved, and we can show (b) similar to the proof of (a). ■

Proof of Theorem 1. Without loss of generality, we assume that $n = K(L+1)$ for some $L \in \mathbb{N}$. We have

$$\begin{aligned}
|\hat{T}_{ij,\theta}^\alpha - T_{ij}| &\leq \left| \frac{1}{(n-K)\theta_{ij}} \sum_{k=1}^{n-K} \psi_{\alpha_{ij}} \{ \theta_{ij} Q_{ij}^c(\tau_k) \} - T_{ij} \right| \\
&\quad + \left| \frac{1}{(n-K)\theta_{ij}} \sum_{k=1}^{n-K} \left[\psi_{\alpha_{ij}} \{ \theta_{ij} Q_{ij}(\tau_k) \} - \psi_{\alpha_{ij}} \{ \theta_{ij} Q_{ij}^c(\tau_k) \} \right] \right| \\
&= (I) + (II).
\end{aligned} \tag{A.3}$$

First, consider (I). Let

$$A_{ij}(\tau_k) = \mathbb{E} \left[Q_{ij}^c(\tau_k) \middle| \mathcal{F}_{\tau_k} \right].$$

Then for any $s > 0$, we obtain that

$$\begin{aligned}
&\Pr \left\{ \frac{1}{(n-K)\theta_{ij}} \sum_{k=1}^{n-K} \psi_{\alpha_{ij}} \{ \theta_{ij} Q_{ij}^c(\tau_k) \} - \frac{1}{n-K} \sum_{k=1}^{n-K} A_{ij}(\tau_k) \geq \frac{K}{n-K} s \right\} \\
&\leq \exp \{ -\theta_{ij} s \} \mathbb{E} \left[\prod_{m=0}^{K-1} \prod_{k=0}^{L-1} \exp \left\{ \frac{1}{K} \left[\psi_{\alpha_{ij}} \{ \theta_{ij} Q_{ij}^c(\tau_{Kk+m+1}) \} - \theta_{ij} A_{ij}(\tau_{Kk+m+1}) \right] \right\} \right]^{1/K} \\
&\leq \exp \{ -\theta_{ij} s \} \prod_{m=0}^{K-1} \mathbb{E} \left[\prod_{k=0}^{L-1} \exp \left[\psi_{\alpha_{ij}} \{ \theta_{ij} Q_{ij}^c(\tau_{Kk+m+1}) \} - \theta_{ij} A_{ij}(\tau_{Kk+m+1}) \right] \right]^{1/K} \\
&= \exp \{ -\theta_{ij} s \} \prod_{m=0}^{K-1} \mathbb{E} \left[\prod_{k=0}^{L-2} \exp \left[\psi_{\alpha_{ij}} \{ \theta_{ij} Q_{ij}^c(\tau_{Kk+m+1}) \} - \theta_{ij} A_{ij}(\tau_{Kk+m+1}) \right] \right]
\end{aligned}$$

$$\begin{aligned}
& \times \mathbb{E} \left[\exp \left[\psi_{\alpha_{ij}} \left\{ \theta_{ij} Q_{ij}^c (\tau_{K(L-1)+m+1}) \right\} - \theta_{ij} A_{ij} (\tau_{K(L-1)+m+1}) \right] \middle| \mathcal{F}_{\tau_{K(L-1)+m+1}} \right]^{1/K} \\
& \leq \exp \left\{ -\theta_{ij} s \right\} \prod_{m=0}^{K-1} \mathbb{E} \left[\prod_{k=0}^{L-2} \exp \left[\psi_{\alpha_{ij}} \left\{ \theta_{ij} Q_{ij}^c (\tau_{Kk+m+1}) \right\} - \theta_{ij} A_{ij} (\tau_{Kk+m+1}) \right] \right]^{1/K} \\
& \quad \times \exp \left\{ K^{-1} \sum_{m=0}^{K-1} c_{\alpha_{ij}} U_{ij} (\tau_{K(L-1)+m+1}) \theta_{ij}^{\alpha_{ij}} \right\} \\
& \leq \exp \left\{ -\theta_{ij} s + \frac{n-K}{K} c_{\alpha_{ij}} S_{ij} \theta_{ij}^{\alpha_{ij}} \right\}, \tag{A.4}
\end{aligned}$$

where the first and second inequalities are due to the Markov inequality and Hölder's inequality, respectively, and the third and fourth inequalities can be obtained by (A.5). Since we can get $-\log(1 - x + c_{\alpha_{ij}}|x|^{\alpha_{ij}}) \leq \psi_{\alpha_{ij}}(x) \leq \log(1 + x + c_{\alpha_{ij}}|x|^{\alpha_{ij}})$ from Lemma A.2 (Minsker, 2018), we have

$$\begin{aligned}
& \mathbb{E} \left[\exp \left[\psi_{\alpha_{ij}} \left\{ \theta_{ij} Q_{ij}^c (\tau_k) \right\} - \theta_{ij} A_{ij} (\tau_k) \right] \middle| \mathcal{F}_{\tau_k} \right] \\
& \leq \mathbb{E} \left[\exp \left[\log \left\{ 1 + \theta_{ij} Q_{ij}^c (\tau_k) + c_{\alpha_{ij}} |\theta_{ij} Q_{ij}^c (\tau_k)|^{\alpha_{ij}} \right\} - \theta_{ij} A_{ij} (\tau_k) \right] \middle| \mathcal{F}_{\tau_k} \right] \\
& = \exp \left[\log \left\{ 1 + \theta_{ij} A_{ij} (\tau_k) + c_{\alpha_{ij}} \theta_{ij}^{\alpha_{ij}} \mathbb{E} [|Q_{ij}^c(\tau_k)|^{\alpha_{ij}} | \mathcal{F}_{\tau_k}] \right\} - \theta_{ij} A_{ij} (\tau_k) \right] \\
& \leq \exp \left[c_{\alpha_{ij}} \theta_{ij}^{\alpha_{ij}} \mathbb{E} [|Q_{ij}^c(\tau_k)|^{\alpha_{ij}} | \mathcal{F}_{\tau_k}] \right] \leq \exp \left[c_{\alpha_{ij}} U_{ij} (\tau_k) \theta_{ij}^{\alpha_{ij}} \right] \text{ a.s.}, \tag{A.5}
\end{aligned}$$

where the second inequality is due to the fact that $\log(1 + x) \leq x$ for any $x > -1$, and the last inequality is from Proposition 2. Choose

$$\theta_{ij} = \left(\frac{K_n \log y^{-1}}{(\alpha_{ij} - 1) c_{\alpha_{ij}} S_{ij} (n - K_n)} \right)^{1/\alpha_{ij}}, \quad s = \left(\frac{\alpha_{ij}^{\alpha_{ij}} c_{\alpha_{ij}} S_{ij} (n - K) (\log y^{-1})^{\alpha_{ij}-1}}{(\alpha_{ij} - 1)^{\alpha_{ij}-1} K} \right)^{1/\alpha_{ij}},$$

where $c \log n \leq \log y^{-1} \leq 2\sqrt{n}$. Then we have

$$\begin{aligned}
& \Pr \left[\frac{1}{(n - K) \theta_{ij}} \sum_{k=1}^{n-K} \psi_{\alpha_{ij}} \left\{ \theta_{ij} Q_{ij}^c (\tau_k) \right\} - \frac{1}{n - K} \sum_{k=0}^{n-K} A_{ij} (\tau_k) \right. \\
& \quad \left. \geq \left(\frac{\alpha_{ij}^{\alpha_{ij}} c_{\alpha_{ij}} S_{ij} K^{\alpha_{ij}-1} (\log y^{-1})^{\alpha_{ij}-1}}{(\alpha_{ij} - 1)^{\alpha_{ij}-1} (n - K)^{\alpha_{ij}-1}} \right)^{1/\alpha_{ij}} \right] \leq y.
\end{aligned}$$

Similarly, we can show

$$\Pr \left[\left| \frac{1}{(n-K)\theta_{ij}} \sum_{k=1}^{n-K} \psi_{\alpha_{ij}} \{ \theta_{ij} Q_{ij}^c(\tau_k) \} - \frac{1}{n-K} \sum_{k=0}^{n-K} A_{ij}(\tau_k) \right| \leq C (n^{-1/2} \log y^{-1})^{(\alpha_{ij}-1)/\alpha_{ij}} \right] \geq 1 - 2y. \quad (\text{A.6})$$

Now, we need to establish the relationship between $\sum_{k=0}^{n-K} A_{ij}(\tau_k)/(n-K)$ and T_{ij} . Since X and ϵ are independent, we have

$$\begin{aligned} A_{ij}(\tau_k) &= \mathbb{E} \left[\bar{X}_i^\mu(\tau_k) \bar{X}_j^\mu(\tau_k) \middle| \mathcal{F}_{\tau_k} \right] + \mathbb{E} \left[\bar{X}_i^\mu(\tau_k) \bar{X}_j^\sigma(\tau_k) + \bar{X}_i^\sigma(\tau_k) \bar{X}_j^\mu(\tau_k) \middle| \mathcal{F}_{\tau_k} \right] \\ &\quad + \mathbb{E} \left[\bar{X}_i^\sigma(\tau_k) \bar{X}_j^\sigma(\tau_k) \middle| \mathcal{F}_{\tau_k} \right] + \mathbb{E} \left[\bar{\epsilon}_i(\tau_k) \bar{\epsilon}_j(\tau_k) \middle| \mathcal{F}_{\tau_k} \right] \\ &= (a) + (b) + (c) + (d). \end{aligned}$$

By the fact that $|\bar{X}_i^\mu(\tau_k)| \leq Cn^{-1/4}$ a.s., we have

$$|(a)| \leq Cn^{-1/2} \text{ a.s.} \quad (\text{A.7})$$

Using the Burkholder-Davis-Gundy inequality, we can show

$$|(b)| \leq Cn^{-1/4} \left(\sqrt{\mathbb{E} \left[\{ \bar{X}_i^\sigma(\tau_k) \}^2 \middle| \mathcal{F}_{\tau_k} \right]} + \sqrt{\mathbb{E} \left[\{ \bar{X}_j^\sigma(\tau_k) \}^2 \middle| \mathcal{F}_{\tau_k} \right]} \right) \leq Cn^{-1/4} \text{ a.s.} \quad (\text{A.8})$$

Consider (c). Let

$$\bar{X}_i^\sigma(\tau_k) = \sqrt{\frac{n-K}{\phi K}} \sum_{l=0}^{K-1} H_{i,k,l},$$

where

$$\begin{aligned} H_{i,k,l} &= g \left(\frac{l}{K} \right) \int_{\tau_{k+l}}^{\tau_{i,k+l+1}} e_i^\top \boldsymbol{\sigma}^\top(t) d\mathbf{W}_t + g \left(\frac{l+1}{K} \right) \int_{\tau_{i,k+l+1}}^{\tau_{k+l+1}} e_i^\top \boldsymbol{\sigma}^\top(t) d\mathbf{W}_t \\ &= g \left(\frac{l}{K} \right) \int_{\tau_{k+l}}^{\tau_{k+l+1}} e_i^\top \boldsymbol{\sigma}^\top(t) d\mathbf{W}_t + \left\{ g \left(\frac{l+1}{K} \right) - g \left(\frac{l}{K} \right) \right\} \int_{\tau_{i,k+l+1}}^{\tau_{k+l+1}} e_i^\top \boldsymbol{\sigma}^\top(t) d\mathbf{W}_t. \end{aligned}$$

Then we have

$$(c) = \frac{n-K}{\phi K} \sum_{l=0}^{K-1} \mathbb{E} \left[H_{i,k,l} H_{j,k,l} \middle| \mathcal{F}_{\tau_k} \right] \text{ a.s.}$$

By the Itô's isometry and the boundedness of $\gamma_{ij}(t)$, we can get for all $0 \leq l \leq K-1$,

$$\begin{aligned} & \mathbb{E} \left[H_{i,k,l} H_{j,k,l} \middle| \mathcal{F}_{\tau_k} \right] - \left\{ g \left(\frac{l}{K} \right) \right\}^2 \mathbb{E} \left\{ \int_{\tau_{k+l}}^{\tau_{k+l+1}} \gamma_{ij}(t) dt \middle| \mathcal{F}_{\tau_k} \right\} \\ & \leq Cn^{-1} \left[\left\{ g \left(\frac{l+1}{K} \right) - g \left(\frac{l}{K} \right) \right\}^2 + \left| g \left(\frac{l}{K} \right) \left\{ g \left(\frac{l+1}{K} \right) - g \left(\frac{l}{K} \right) \right\} \right| \right] \\ & \leq Cn^{-3/2} \text{ a.s.}, \end{aligned}$$

where the last inequality is by the piecewise Lipschitz derivative condition for $g(\cdot)$. Thus, we have

$$\left| (c) - \frac{n-K}{\phi K} \sum_{l=0}^{K-1} \left\{ g \left(\frac{l}{K} \right) \right\}^2 \mathbb{E} \left\{ \int_{\tau_{k+l}}^{\tau_{k+l+1}} \gamma_{ij}(t) dt \middle| \mathcal{F}_{\tau_k} \right\} \right| \leq Cn^{-1/2} \text{ a.s.} \quad (\text{A.9})$$

Finally, for (d), we have

$$(d) = \frac{n-K}{\phi K} \sum_{l=0}^{K-1} \left\{ g \left(\frac{l}{K} \right) - g \left(\frac{l+1}{K} \right) \right\}^2 \mathbf{1}(\tau_{i,k+l+1} = \tau_{j,k+l+1}) \eta_{ij} \text{ a.s.} \quad (\text{A.10})$$

Combining (A.7)–(A.10), we have

$$\left| \frac{1}{n-K} \sum_{k=1}^{n-K} A_{ij}(\tau_k) - A_{ij}^* \right| \leq Cn^{-1/4} \text{ a.s.}, \quad (\text{A.11})$$

where

$$A_{ij}^* = \frac{1}{\phi K} \sum_{l=0}^{K-1} \left\{ g \left(\frac{l}{K} \right) \right\}^2 \sum_{k=1}^{n-K} \mathbb{E} \left\{ \int_{\tau_{k+l}}^{\tau_{k+l+1}} \gamma_{ij}(t) dt \middle| \mathcal{F}_{\tau_k} \right\} + \rho_{ij}.$$

Now, we investigate the relationship between A_{ij}^* and T_{ij} . Note that $\gamma_{ij}(t)$ is bounded and $\sum_{k=1}^{n-K} \left[\mathbb{E} \left\{ \int_{\tau_{k+l}}^{\tau_{k+l+1}} \gamma_{ij}(t) dt \middle| \mathcal{F}_{\tau_k} \right\} - \int_{\tau_{k+l}}^{\tau_{k+l+1}} \gamma_{ij}(t) dt \right]$ is the sum of $l+1$ martingales. Hence,

using the Azuma-Hoeffding inequality for each martingale, we can show for all $0 \leq l \leq K-1$,

$$\Pr \left(\left| \sum_{k=1}^{n-K} \left[\mathbb{E} \left\{ \int_{\tau_{k+l}}^{\tau_{k+l+1}} \gamma_{ij}(t) dt \middle| \mathcal{F}_{\tau_k} \right\} - \int_{\tau_{k+l}}^{\tau_{k+l+1}} \gamma_{ij}(t) dt \right] \right| \geq C (n^{-1/2} \log y^{-1})^{1/2} \right) \leq Ky.$$

Also, simple algebraic manipulations show

$$\begin{aligned} & |A_{ij}^* - T_{ij}| \\ &= \left| \frac{1}{\phi K} \sum_{l=0}^{K-1} \left\{ g \left(\frac{l}{K} \right) \right\}^2 \left(\left[\sum_{k=1}^{n-K} \mathbb{E} \left\{ \int_{\tau_{k+l}}^{\tau_{k+l+1}} \gamma_{ij}(t) dt \middle| \mathcal{F}_{\tau_k} \right\} \right] - \int_0^1 \gamma_{ij}(t) dt \right) \right| \\ &\leq \left| \frac{1}{\phi K} \sum_{l=0}^{K-1} \left\{ g \left(\frac{l}{K} \right) \right\}^2 \sum_{k=1}^{n-K} \left[\mathbb{E} \left\{ \int_{\tau_{k+l}}^{\tau_{k+l+1}} \gamma_{ij}(t) dt \middle| \mathcal{F}_{\tau_k} \right\} - \int_{\tau_{k+l}}^{\tau_{k+l+1}} \gamma_{ij}(t) dt \right] \right| + 2 \frac{K}{n} \nu_{\gamma}. \end{aligned}$$

Therefore, we have

$$\Pr \left\{ |A_{ij}^* - T_{ij}| \leq C (n^{-1/2} \log y^{-1})^{1/2} + 2 \frac{K}{n} \nu_{\gamma} \right\} \geq 1 - K^2 y. \quad (\text{A.12})$$

Combining (A.6), (A.11), and (A.12), we have

$$\Pr \left\{ (I) \leq C (n^{-1/2} \log y^{-1})^{(\alpha_{ij}-1)/\alpha_{ij}} \right\} \geq 1 - 2K^2 y. \quad (\text{A.13})$$

Consider (II). Note that by the boundedness of the intensity, we have

$$\Pr \left\{ \Lambda_i(1) \leq C \log y^{-1} \right\} \geq 1 - y.$$

Hence, using the fact that $\psi_{\alpha}(x)$ is a bounded function, we have

$$\Pr \left\{ (II) \leq C \left(\frac{K \log y^{-1}}{n \theta_{ij}} \right) \right\} \geq 1 - 2y,$$

which implies

$$\Pr \left\{ (II) \leq C (n^{-1/2} \log y^{-1})^{(\alpha_{ij}-1)/\alpha_{ij}} \right\} \geq 1 - 2y. \quad (\text{A.14})$$

Collecting (A.3), (A.13), and (A.14), we obtain that with probability at least $1 - 3K^2y$,

$$|\widehat{T}_{ij,\theta}^\alpha - T_{ij}| \leq C \left(n^{-1/2} \log y^{-1} \right)^{(\alpha_{ij}-1)/\alpha_{ij}},$$

and then substituting $\delta/(3K^2)$ for y completes the proof. ■

A.2 Proof of Theorem 2

Proof of Theorem 2. Let $n_i = n_j = n$ and $t_{i,k} = t_{j,k} = \tau_{i,k} = \tau_{j,k} = \tau_k = k/n$ for $1 \leq k \leq n$. To derive a lower bound, we construct two quadratic pre-averaged random variables $Q_{1,ij}(\tau_k)$ and $Q_{2,ij}(\tau_k)$ as follows. Let $d\mathbf{X}_1(t) = d\mathbf{X}_2(t) = \boldsymbol{\sigma}^\top(t)d\mathbf{W}_t$ for any appropriate $\boldsymbol{\sigma}(t)$, which implies $\bar{X}_{1,h}(\tau_k) = \bar{X}_{2,h}(\tau_k)$ for $1 \leq h \leq p$ and $1 \leq k \leq n-K$. Also, let $2\epsilon_{1,h}(t_{h,k}) = \epsilon_{2,h}(t_{h,k})$ for $1 \leq h \leq p$ and $0 \leq k \leq n$, where the distributions of $\epsilon_{1,h}(t_{h,k})$, $1 \leq h \leq p$ are defined as follows:

$$\epsilon_{1,h}(t_{h,k}) = \begin{cases} K^{(\alpha_h+1)/2\alpha_h} (\log(1/2\delta))^{-1/2\alpha_h} & \text{with probability } d \\ 0 & \text{with probability } 1-2d \\ -K^{(\alpha_h+1)/2\alpha_h} (\log(1/2\delta))^{-1/2\alpha_h} & \text{with probability } d, \end{cases}$$

where $d = C_K^2 \log(1/2\delta)/4K^2$. For each $0 \leq k \leq n$, let $\Pr\{\epsilon_{1,h}(t_{h,k}) > 0 \text{ for all } 1 \leq h \leq p\} = \Pr\{\epsilon_{1,h}(t_{h,k}) < 0 \text{ for all } 1 \leq h \leq p\} = d$ and $\Pr\{\epsilon_{1,h}(t_{h,k}) = 0 \text{ for all } 1 \leq h \leq p\} = 1-2d$. Then, using the fact that $1-x \geq \exp(-x/(1-x))$ for any $0 \leq x \leq 1/2$, we can show

$$\prod_{k=1}^n \Pr\{\epsilon_{1,i}(\tau_k) = \epsilon_{1,j}(\tau_k) = \epsilon_{2,i}(\tau_k) = \epsilon_{2,j}(\tau_k) = 0\} = \left(1 - \frac{1}{2n} \log \frac{1}{2\delta}\right)^n \geq 2\delta. \quad (\text{A.15})$$

Here, we need to check whether the construction satisfies Assumption 1(c). It suffices to show

$$\mathbb{E} [|Q_{1,ii}^c(\tau_1)|^{\alpha_i}] \leq C. \quad (\text{A.16})$$

Note that for all $1 \leq k \leq n$,

$$\mathbb{E} [|\epsilon_{1,i}(\tau_k)|^{2\alpha_i}] = \frac{C_K^2}{2} K^{\alpha_i-1} \quad \text{and} \quad \mathbb{E} [\epsilon_{1,i}^2(\tau_k)] = \frac{C_K^2}{2} \left(K^{-1} \log \frac{1}{2\delta} \right)^{(\alpha_i-1)/\alpha_i}.$$

Hence, by the Lipschitz continuity of $g(\cdot)$, we have

$$\begin{aligned} \mathbb{E} [|\bar{\epsilon}_{1,i}(\tau_1)|^{2\alpha_i}] &= \left(\sqrt{\frac{n-K}{\phi K}} \frac{1}{K} \right)^{2\alpha_i} \mathbb{E} \left[\left| \sum_{l=0}^{K-1} K \left\{ g\left(\frac{l}{K}\right) - g\left(\frac{l+1}{K}\right) \right\} \epsilon_{1,i}(\tau_{l+2}) \right|^{2\alpha_i} \right] \\ &\leq CK^{-\alpha_i} \left\{ \sum_{l=0}^{K-1} \mathbb{E} [|\epsilon_{1,i}(\tau_{l+2})|^{2\alpha_i}] + \left(\sum_{l=0}^{K-1} \mathbb{E} [\epsilon_{1,i}^2(\tau_{l+2})] \right)^{\alpha_i} \right\} \\ &\leq C + CK^{-\alpha_i} \left\{ K \left(K^{-1} \log \frac{1}{2\delta} \right)^{(\alpha_i-1)/\alpha_i} \right\}^{\alpha_i} \leq C, \end{aligned} \quad (\text{A.17})$$

where the first inequality is due to the Rosenthal's inequality. Then similar to the proof of Proposition 2, we can show (A.16).

Now, since

$$|T_{1,ij} - T_{2,ij}| = \frac{3n\zeta}{\phi K} \mathbb{E} [\epsilon_{1,i}(\tau_1) \epsilon_{1,j}(\tau_1)],$$

we have for any $\widehat{T}_{ij}(Q_{ij}(\tau_k), \delta)$,

$$\begin{aligned} &\max \left[\Pr \left\{ \left| \widehat{T}_{ij}(Q_{1,ij}(\tau_k), \delta) - T_{1,ij} \right| \geq \frac{n\zeta}{\phi K} \mathbb{E} [\epsilon_{1,i}(\tau_1) \epsilon_{1,j}(\tau_1)] \right\}, \right. \\ &\quad \left. \Pr \left\{ \left| \widehat{T}_{ij}(Q_{2,ij}(\tau_k), \delta) - T_{2,ij} \right| \geq \frac{n\zeta}{\phi K} \mathbb{E} [\epsilon_{1,i}(\tau_1) \epsilon_{1,j}(\tau_1)] \right\} \right] \\ &\geq \frac{1}{2} \Pr \left[\left| \widehat{T}_{ij}(Q_{1,ij}(\tau_k), \delta) - T_{1,ij} \right| \geq \frac{n\zeta}{\phi K} \mathbb{E} [\epsilon_{1,i}(\tau_1) \epsilon_{1,j}(\tau_1)] \right. \\ &\quad \left. \text{or} \quad \left| \widehat{T}_{ij}(Q_{2,ij}(\tau_k), \delta) - T_{2,ij} \right| \geq \frac{n\zeta}{\phi K} \mathbb{E} [\epsilon_{1,i}(\tau_1) \epsilon_{1,j}(\tau_1)] \right] \\ &\geq \frac{1}{2} \Pr \left\{ \widehat{T}_{ij}(Q_{1,ij}(\tau_k), \delta) = \widehat{T}_{ij}(Q_{2,ij}(\tau_k), \delta) \right\} \\ &\geq \frac{1}{2} \prod_{k=1}^n \Pr \{ \epsilon_{1,i}(\tau_k) = \epsilon_{1,j}(\tau_k) = \epsilon_{2,i}(\tau_k) = \epsilon_{2,j}(\tau_k) = 0 \} \geq \delta, \end{aligned} \quad (\text{A.18})$$

where the last inequality is from (A.15). Combining (A.18) and the fact that $\mathbb{E} [\epsilon_{1,i}(\tau_1) \epsilon_{1,j}(\tau_1)] = C (K^{-1} \log(1/2\delta))^{(\alpha_{ij}-1)/\alpha_{ij}}$, we have for sufficiently large n ,

$$\begin{aligned} & \max \left[\Pr \left\{ \left| \widehat{T}_{ij}(Q_{1,ij}(\tau_k), \delta) - T_{1,ij} \right| \geq C \left(n^{-1/2} \log \frac{1}{2\delta} \right)^{(\alpha_{ij}-1)/\alpha_{ij}} \right\}, \right. \\ & \quad \left. \Pr \left\{ \left| \widehat{T}_{ij}(Q_{2,ij}(\tau_k), \delta) - T_{2,ij} \right| \geq C \left(n^{-1/2} \log \frac{1}{2\delta} \right)^{(\alpha_{ij}-1)/\alpha_{ij}} \right\} \right] \\ & \geq \delta, \end{aligned} \tag{A.19}$$

which completes the proof. ■

A.3 Proof of Theorem 3

Proposition 3. *Under Assumption 1(a)–(b) and Assumption 2, Assumption 1(c) is satisfied.*

Proof of Proposition 3. Similar to the proof of Proposition 2, we can show

$$\mathbb{E} [|\epsilon_i(\tau_{i,k})|^{2\alpha_i}] \leq C.$$

Then we have

$$\begin{aligned} \mathbb{E} [|Q_{ii}^c(\tau_k)|^{\alpha_i}] &= \mathbb{E} \left[\left| \bar{X}_i^\mu(\tau_k) + \bar{X}_i^\sigma(\tau_k) + \bar{\epsilon}_i(\tau_k) \right|^{2\alpha_i} \right] \\ &\leq C + C \mathbb{E} \left[\left| \bar{X}_i^\sigma(\tau_k) \right|^{2\alpha_i} \right] + C \mathbb{E} \left[\left| \bar{\epsilon}_i(\tau_k) \right|^{2\alpha_i} \right] \\ &\leq C + C \left| \frac{n-K}{\phi K} \sum_{l=0}^{K-1} g^2 \left(\frac{l}{K} \right) \frac{\nu_\gamma}{n} \right|^{\alpha_i} \\ &\quad + C \mathbb{E} \left[\left| \frac{n-K}{\phi K} \sum_{l=0}^{K-1} \left\{ g \left(\frac{l}{K} \right) - g \left(\frac{l+1}{K} \right) \right\}^2 \epsilon_i^2(\tau_{i,k+l+1}) \right|^{\alpha_i} \right] \\ &\leq C + C K^{-\alpha_i} \mathbb{E} \left[\left| \sum_{l=0}^{K-1} \epsilon_i^2(\tau_{i,k+l+1}) \right|^{\alpha_i} \right] \\ &\leq C + C K^{-1} \sum_{l=0}^{K-1} \mathbb{E} [|\epsilon_i(\tau_{i,k+l+1})|^{2\alpha_i}] \leq C \text{ a.s.}, \end{aligned}$$

where the first and fourth inequalities are due to the Hölder's inequality, and the second inequality is from the Burkholder-Davis-Gundy inequality. ■

Proof of Theorem 3. Without loss of generality, we assume that $n = 2L + 1$ for some $L \in \mathbb{N}$. We have

$$\begin{aligned} |\widehat{\rho}_{ij,\theta}^\alpha - \rho_{ij}| &\leq \left| \frac{\zeta}{\phi K \theta_{\rho,ij}} \sum_{k=1}^{n-1} \psi_{\alpha_{ij}} \{ \theta_{\rho,ij} Q_{\rho,ij}^c(\tau_k) \} - \rho_{ij} \right| \\ &\quad + \left| \frac{\zeta}{\phi K \theta_{\rho,ij}} \sum_{k=1}^{n-1} \left[\psi_{\alpha_{ij}} \{ \theta_{\rho,ij} Q_{\rho,ij}(\tau_k) \} - \psi_{\alpha_{ij}} \{ \theta_{\rho,ij} Q_{\rho,ij}^c(\tau_k) \} \right] \right| \\ &= (I) + (II). \end{aligned} \quad (\text{A.20})$$

First, consider (I) . Let

$$(\zeta / \phi K \theta_{\rho,ij}) \sum_{k=1}^{n-1} \psi_{\alpha_{ij}} \{ \theta_{\rho,ij} Q_{\rho,ij}^c(\tau_k) \} = \widehat{\rho}_{1,ij,\theta}^{\alpha,c} + \widehat{\rho}_{2,ij,\theta}^{\alpha,c},$$

where

$$\begin{aligned} \widehat{\rho}_{1,ij,\theta}^{\alpha,c} &= \frac{\zeta}{\phi K \theta_{\rho,ij}} \sum_{k=1}^L \psi_{\alpha_{ij}} \{ \theta_{\rho,ij} Q_{\rho,ij}^c(\tau_{2k-1}) \}, \\ \widehat{\rho}_{2,ij,\theta}^{\alpha,c} &= \frac{\zeta}{\phi K \theta_{\rho,ij}} \sum_{k=1}^L \psi_{\alpha_{ij}} \{ \theta_{\rho,ij} Q_{\rho,ij}^c(\tau_{2k}) \}. \end{aligned}$$

Also, define

$$A_{\rho,ij}(\tau_k) = \mathbb{E} \left[Q_{\rho,ij}^c(\tau_k) \mid \mathcal{F}_{\tau_{k-1}} \right].$$

Then we can show for any $s > 0$,

$$\begin{aligned} &\Pr \left\{ \widehat{\rho}_{1,ij,\theta}^{\alpha,c} - \frac{\zeta}{\phi K} \sum_{k=1}^L A_{\rho,ij}(\tau_{2k-1}) \geq \frac{\zeta s}{\phi K} \right\} \\ &\leq \exp \{ -\theta_{\rho,ij} s \} \mathbb{E} \left[\exp \left\{ \sum_{k=1}^L \left[\psi_{\alpha_{ij}} \{ \theta_{\rho,ij} Q_{\rho,ij}^c(\tau_{2k-1}) \} - \theta_{\rho,ij} A_{\rho,ij}(\tau_{2k-1}) \right] \right\} \right] \\ &= \exp \{ -\theta_{\rho,ij} s \} \mathbb{E} \left[\exp \left\{ \sum_{k=1}^{L-1} \left[\psi_{\alpha_{ij}} \{ \theta_{\rho,ij} Q_{\rho,ij}^c(\tau_{2k-1}) \} - \theta_{\rho,ij} A_{\rho,ij}(\tau_{2k-1}) \right] \right\} \right] \end{aligned}$$

$$\begin{aligned}
& \times \mathbb{E} \left[\exp \left[\psi_{\alpha_{ij}} \left\{ \theta_{\rho,ij} Q_{\rho,ij}^c(\tau_{2L-1}) \right\} - \theta_{\rho,ij} A_{\rho,ij}(\tau_{2L-1}) \right] \middle| \mathcal{F}_{\tau_{2L-2}} \right] \\
& \leq \exp \left\{ -\theta_{\rho,ij} s \right\} \mathbb{E} \left[\exp \left\{ \sum_{k=1}^{L-1} \left[\psi_{\alpha_{ij}} \left\{ \theta_{\rho,ij} Q_{\rho,ij}^c(\tau_{2k-1}) \right\} - \theta_{\rho,ij} A_{\rho,ij}(\tau_{2k-1}) \right] \right\} \right. \\
& \quad \times \left. \exp \left\{ c_{\alpha_{ij}} U_{\rho,ij}(\tau_{2L-2}) \theta_{\rho,ij}^{\alpha_{ij}} \right\} \right] \\
& \leq \exp \left\{ -\theta_{\rho,ij} s + (n-1) c_{\alpha_{ij}} S_{\rho,ij} \theta_{\rho,ij}^{\alpha_{ij}} \right\}.
\end{aligned}$$

Choose

$$\theta_{\rho,ij} = \left(\frac{\log y^{-1}}{(\alpha_{ij} - 1) c_{\alpha_{ij}} S_{\rho,ij} (n-1)} \right)^{1/\alpha_{ij}}, \quad s = \left(\frac{\alpha_{ij}^{\alpha_{ij}} c_{\alpha_{ij}} S_{\rho,ij} (n-1) (\log y^{-1})^{\alpha_{ij}-1}}{(\alpha_{ij} - 1)^{\alpha_{ij}-1}} \right)^{1/\alpha_{ij}},$$

where $c \log n \leq \log y^{-1} \leq 2\sqrt{n}$. Then we have

$$\Pr \left\{ \widehat{\rho}_{1,ij,\theta}^{\alpha,c} - \frac{\zeta}{\phi K} \sum_{k=1}^L A_{\rho,ij}(\tau_{2k-1}) \geq C (n^{-1} \log y^{-1})^{(\alpha_{ij}-1)/\alpha_{ij}} \right\} \leq y.$$

Similarly, we can show

$$\Pr \left[\left| \frac{\zeta}{\phi K \theta_{\rho,ij}} \sum_{k=1}^{n-1} \psi_{\alpha_{ij}} \left\{ \theta_{\rho,ij} Q_{\rho,ij}^c(\tau_k) \right\} - \frac{\zeta}{\phi K} \sum_{k=1}^{n-1} A_{\rho,ij}(\tau_k) \right| \geq C (n^{-1} \log y^{-1})^{(\alpha_{ij}-1)/\alpha_{ij}} \right] \leq 4y. \quad (\text{A.21})$$

Now, we need to establish the relationship between $\zeta \sum_{k=1}^{n-1} A_{\rho,ij}(\tau_k) / (\phi K)$ and ρ_{ij} . Since X and ϵ are independent, similar to the proof of Theorem 1, we can show

$$\left| \rho_{ij} - \frac{\zeta}{\phi K} \sum_{k=1}^{n-1} A_{\rho,ij}(\tau_k) \right| \leq C n^{-1} \text{ a.s.} \quad (\text{A.22})$$

Combining (A.21) and (A.22), we have

$$\Pr \left\{ (I) \leq C (n^{-1} \log y^{-1})^{(\alpha_{ij}-1)/\alpha_{ij}} \right\} \geq 1 - 4y. \quad (\text{A.23})$$

Consider (II). Note that

$$\Pr \{ \Lambda_i(1) \leq C \log y^{-1} \} \geq 1 - y.$$

Hence, using the fact that $\psi_\alpha(x)$ is a bounded function, we have

$$\Pr \left\{ (II) \leq C \left(\frac{\log y^{-1}}{n\theta_{\rho,ij}} \right) \right\} \geq 1 - 2y,$$

which implies

$$\Pr \left\{ (II) \leq C \left(n^{-1} \log y^{-1} \right)^{(\alpha_{ij}-1)/\alpha_{ij}} \right\} \geq 1 - 2y. \quad (\text{A.24})$$

Collecting (A.20), (A.23), and (A.24), we obtain that with probability at least $1 - 6y$,

$$|\hat{\rho}_{ij,\theta}^\alpha - \rho_{ij}| \leq C \left(n^{-1} \log y^{-1} \right)^{(\alpha_{ij}-1)/\alpha_{ij}},$$

and then substituting $\delta/6$ for y completes the proof of (4.4). Also, (4.5) is proved by (4.3) and Theorem 1. ■

A.4 Proof of Theorem 4

Proof of Theorem 4. Let $n_i = n_j = n$ and $t_{i,k} = t_{j,k} = \tau_{i,k} = \tau_{j,k} = \tau_k = k/n$ for $1 \leq k \leq n$. Similar to the proof of Theorem 2, we construct two quadratic log-return random variables $Q_{1,\rho,ij}(\tau_k)$ and $Q_{2,\rho,ij}(\tau_k)$ as follows. Let $d\mathbf{X}_1(t) = d\mathbf{X}_2(t) = \boldsymbol{\sigma}^\top(t)d\mathbf{W}_t$ for any appropriate $\boldsymbol{\sigma}(t)$, which implies $X_{1,h}(\tau_{k+1}) - X_{1,h}(\tau_k) = X_{2,h}(\tau_{k+1}) - X_{2,h}(\tau_k)$ for $1 \leq h \leq p$ and $1 \leq k \leq n-1$. Also, let $2\epsilon_{1,h}(t_{h,k}) = \epsilon_{2,h}(t_{h,k})$ for $1 \leq h \leq p$ and $0 \leq k \leq n$, where the distributions of $\epsilon_{1,h}(t_{h,k})$, $1 \leq h \leq p$ are defined as follows:

$$\epsilon_{1,h}(t_{h,k}) = \begin{cases} n^{1/2\alpha_h} (\log(1/2\delta))^{-1/2\alpha_h} & \text{with probability } d \\ 0 & \text{with probability } 1 - 2d \\ -n^{1/2\alpha_h} (\log(1/2\delta))^{-1/2\alpha_h} & \text{with probability } d, \end{cases}$$

where $d = \log(1/2\delta)/8n$. For each $0 \leq k \leq n$, let $\Pr \{ \epsilon_{1,h}(t_{h,k}) > 0 \text{ for all } 1 \leq h \leq p \} = \Pr \{ \epsilon_{1,h}(t_{h,k}) < 0 \text{ for all } 1 \leq h \leq p \} = d$ and $\Pr \{ \epsilon_{1,h}(t_{h,k}) = 0 \text{ for all } 1 \leq h \leq p \} = 1 - 2d$. Then, using the fact that $1 - x \geq \exp(-x/(1-x))$ for any $0 \leq x \leq 1/2$, we can show

$$\prod_{k=1}^n \Pr \{ \epsilon_{1,i}(\tau_k) = \epsilon_{1,j}(\tau_k) = \epsilon_{2,i}(\tau_k) = \epsilon_{2,j}(\tau_k) = 0 \} = \left(1 - \frac{1}{4n} \log \frac{1}{2\delta} \right)^n \geq 2\delta. \quad (\text{A.25})$$

Here, we need to check whether the construction satisfies Assumption 2. It suffices to show

$$\mathbb{E} [|\epsilon_{1,i}(\tau_1)|^{2\alpha_i}] \leq C. \quad (\text{A.26})$$

Note that

$$\mathbb{E} [|\epsilon_{1,i}(\tau_1)|^{2\alpha_i}] = \frac{1}{4} \quad \text{and} \quad \mathbb{E} [\epsilon_{1,i}(\tau_1) \epsilon_{1,j}(\tau_1)] = \frac{1}{4} \left(n^{-1} \log \frac{1}{2\delta} \right)^{(\alpha_{ij}-1)/\alpha_{ij}}.$$

Hence, (A.26) is satisfied, and since

$$|\rho_{1,ij} - \rho_{2,ij}| = \frac{3n\zeta}{\phi K} \mathbb{E} [\epsilon_{1,i}(\tau_1) \epsilon_{1,j}(\tau_1)],$$

we have for any $\widehat{\rho}_{ij}(Q_{\rho,ij}(\tau_k), \delta)$,

$$\begin{aligned} & \max \left[\Pr \left\{ |\widehat{\rho}_{ij}(Q_{1,\rho,ij}(\tau_k), \delta) - \rho_{1,ij}| \geq \frac{n\zeta}{4\phi K} \left(n^{-1} \log \frac{1}{2\delta} \right)^{(\alpha_{ij}-1)/\alpha_{ij}} \right\}, \right. \\ & \quad \Pr \left\{ |\widehat{\rho}_{ij}(Q_{2,\rho,ij}(\tau_k), \delta) - \rho_{2,ij}| \geq \frac{n\zeta}{4\phi K} \left(n^{-1} \log \frac{1}{2\delta} \right)^{(\alpha_{ij}-1)/\alpha_{ij}} \right\} \left. \right] \\ & \geq \frac{1}{2} \Pr \left[|\widehat{\rho}_{ij}(Q_{1,\rho,ij}(\tau_k), \delta) - \rho_{1,ij}| \geq \frac{n\zeta}{4\phi K} \left(n^{-1} \log \frac{1}{2\delta} \right)^{(\alpha_{ij}-1)/\alpha_{ij}} \right. \\ & \quad \left. \text{or } |\widehat{\rho}_{ij}(Q_{2,\rho,ij}(\tau_k), \delta) - \rho_{2,ij}| \geq \frac{n\zeta}{4\phi K} \left(n^{-1} \log \frac{1}{2\delta} \right)^{(\alpha_{ij}-1)/\alpha_{ij}} \right] \\ & \geq \frac{1}{2} \Pr \{ \widehat{\rho}_{ij}(Q_{1,\rho,ij}(\tau_k), \delta) = \widehat{\rho}_{ij}(Q_{2,\rho,ij}(\tau_k), \delta) \} \\ & \geq \frac{1}{2} \prod_{k=0}^n \Pr \{ \epsilon_{1,i}(\tau_k) = \epsilon_{1,j}(\tau_k) = \epsilon_{2,i}(\tau_k) = \epsilon_{2,j}(\tau_k) = 0 \} \geq \delta, \end{aligned} \quad (\text{A.27})$$

where the last inequality is from (A.25). ■